

H-SAF Associated Scientist Program
SM_VS11_02

COMPARISON BETWEEN H-SAF
LARGE SCALE SURFACE SOIL MOISTURE,
H-SAF ASSIMILATED SOIL MOISTURE AND
SMOS LEVEL 2 SOIL MOISTURE

Claire Gruhier(1), Clement Albergel(2), Patricia de Rosnay(2),
Stefan Hasenauer(3), Barbara Zeiner(4)

- (1) CESBIO, Toulouse, France
- (2) ECMWF, Reading, UK
- (3) TU Wien, Vienna, Austria
- (4) ZAMG, Vienna, Austria

20 December 2011



Overview of the report

The European Organisation for the Exploitation of Meteorological Satellites (EUMETSAT) Satellite Application Facility on Support to Operational Hydrology and Water Management (H-SAF) was established in late 2005, with the objectives of providing new satellite-derived products for use in operational hydrology, and performing independent validation of these products. H-SAF membership includes 12 EUMETSAT members or cooperating States (Austria, Belgium, Bulgaria, Finland, France, Germany, Hungary, Italy, Poland, Romania, Slovakia and Turkey) and ECMWF (European Centre for Medium-Range Weather Forecasts). The H-SAF is hosted by the Italian Met Service.

In the framework of the H-SAF, the interest for new satellite products focuses on:

- Precipitation rate and cumulate precipitations, including liquid/solid discrimination,
- Soil moisture in the surface layer and in the root zone area,
- Snow parameters such as effective cover, wet/dry discrimination, water equivalent.

ECMWF is a contributor to the core soil moisture products.

Within this framework, in this report of the H-SAF Visiting Scientist Program (SM-VS11-02), three soil moisture products are compared and evaluated. One analysis from the ECMWF Land Surface Data assimilation system, SM-DAS-2 produced for the Hydrological-SAF, and two remotely sensed soil moisture products, namely the ASCAT (Advanced Scatterometers) SM-OBS-1 product from the ASAF and the SMOS (Soil Moisture Ocean Salinity) Level 2 soil moisture product.

SM-DAS-2 is produced offline at a resolution of 25 km on a Gaussian regular grid using the ECMWF EKF (Extended Kalman Filter) surface analysis in which screen level parameters and ASCAT surface soil moisture index data are assimilated. SM-DAS-2 inherits from the previous volumetric product of the H-SAF development phase, SM-ASS-1. ASCAT SM-OBS-1 surface soil moisture is obtained from active C-band scatterometer measurements. It is provided in near real time by EUMETSAT and hereafter it is referred to as ASCAT. And the SMOS soil moisture product is obtained from passive L-band microwave measurements. SMOS Level 2 product developed at CESBIO is used at a resolution of 25 km in this report.

In situ soil moisture data from more than 200 stations located in Africa, Australia, Europe and United States are used to determine the reliability of three soil moisture

products. Evaluation of the times series as well as of the anomaly values, show good performances of the three products to capture surface soil moisture annual cycle and short term variability. Correlations with in situ data are very satisfactory over most of the investigated sites located in contrasted biomes and climate conditions with averaged values of 0.70 for SM-DAS-2, 0.53 for ASCAT and 0.54 for SMOS. Although radio frequency interference disturbs the natural microwave emission of Earth observed by SMOS in several parts of the world, hence the soil moisture retrieval, performances of SMOS over Australia are very encouraging.

The three soil moisture products are also intercompared at global scale. Based on the 2010 data set soil moisture temporal variation and spatial distribution are shown and compared for the three products. Characteristics, monthly average maps and Hovmöller plots are used to investigate consistency and differences between the products. Quantitative comparison is provided by using correlation, root mean square difference between the products at global scale. Both time series and anomaly time series are compared at global scale. In addition case study regions are selected in five continents to provide regional scale comparisons.

Contents

1	Introduction	1
2	Surface soil moisture products	3
2.1	SMOS	3
2.2	ASCAT SM-OBS-1 product	4
2.3	SM-DAS-2	5
3	In situ soil moisture observations	7
3.1	NCRS-SCAN	7
3.2	SMOSMANIA and SWATMEX	10
3.3	AMMA	10
3.4	OZNET	10
3.5	ISMN soil moisture: REMEDHUS, UDC-SMOS and UMSUOL	11
4	Methods	13
4.1	Harmonisation of the data and metrics used for the local comparison	13
4.2	Harmonisation of the data for the global comparison	13
4.3	Anomalies	15
4.4	Additional metrics for Taylor diagram	15
4.5	Hovmöller plots	15
5	Local comparison	17
5.1	Comparison of the normalised times series	17
5.2	Comparison of the anomaly time-series	22
6	Global comparison	29
6.1	Characteristics	29
6.2	Monthly soil moisture values	30
6.3	Latitudinal variations	30
6.4	Statistic results	35
7	Conclusion	39
	Bibliographie	42

List of Figures

3.1	Location of the different in situ soil moisture stations used in this study, 38 in Australia (OZNET network), 154 within the United States (NCRS-SCAN network), 10 in Western Africa (AMMA network), 21 in southwestern France (SMOSMANIA and SWATMEX networks), 7 in Germany (UDC-SMOS network) and 1 in Italy (UMSUOL).	9
4.1	Global map of volumetric soil moisture at saturation (in m^3m^{-3}), obtained from the dominant type of global soil texture map derived from Food and Agriculture Organization digital soil map. This information is used in this study to convert SM-DAS-2 and ASCAT into volumetric soil moisture products.	14
5.1	Taylor diagram illustrating the statistics of the comparison between SM-DAS-2, ASCAT, SMOS and in situ SSM for a) the REMEDHUS network in Spain, b) the OZNET network in Australia and c) the SMOSMANIA network in France. Yellow circles are for SM-DAS-2, green circles for ASCAT and red circles for SMOS.	20
5.2	Taylor diagram illustrating the statistics of the comparison between a) SM-DAS-2, b) ASCAT, C) SMOS and in situ SSM for the NCRS-SCAN network. Yellow circles are for SM-DAS-2, green circles for ASCAT and red circles for SMOS.	21
5.3	Correlation values between in situ SSM and (from top to bottom) ECMWF SM-DAS-2 product, ASCAT and SMOS for the stations of the NCRS-SCAN network.	23
5.4	Temporal evolution of SSM anomaly time-series at the Creon d'Armagnac station of the SMOSMANIA network in southwestern France for 2010, from top to bottom; ECMWF (SM-DAS-2), ASCAT and SMOS (green dots). In situ anomaly time-series are in red.	25
5.5	(top) correlations between ASCAT and in situ data against correlations between ECMWF SM-DAS-2 and in situ data, then same for SMOS and SM-DAS-2, SMOS and ASCAT. (Bottom) Same as top but for anomaly correlation values instead of normalised time series.	27
6.1	Number of observations (left) and soil moisture standard deviation $m^3.m^{-3}$ (right) for SMOS (top), ASCAT (middle), and SM-DAS-2 (bottom) for 2010.	31

6.2	Minimal soil moisture in $m^3.m^{-3}$ (left) and maximal (right) values for SMOS (top), ASCAT (middle), and SM-DAS-2 (bottom) for 2010.	32
6.3	Monthly mean soil moisture ($m^3.m^{-3}$) for SMOS, ASCAT, and SM-DAS-2 for January, April, and July.	33
6.4	Left: Soil moisture time latitude variations (Hovmöller) for 2010, for SMOS (top), ASCAT (middle), and SM-DAS-2 (bottom). Time axis is represented with a three days moving window, and soil moisture values are longitudinal averaged. Right: Soil moisture latitudinal distribution for Jan-Feb-Mar (blue), Apr-May-Jun (green), Jul-Aug-Sep (yellow), and Oct-Nov-Dec (red). The black lines on the hovmoller plot correspond to the quarterly period.	34
6.5	Global maps correlation (left) and anomaly correlation (right) between the three pairs of products (Top: SMOS-ASCAT, Middle: SMOS-SM-DAS and bottom: ASCAT-SM-DAS).	36
6.6	Global maps RMSD (left) and number of day with available values from both products (right) between the three pairs of products (Top: SMOS-ASCAT, Middle: SMOS-SM-DAS and bottom: ASCAT-SM-DAS).	37
6.7	Selected area for regional scale comparison (cf. Table 6.1).	38

List of Tables

3.1	Presentation of the different soil moisture data sets used in this study. NWP stands for numerical weather prediction. 252 stations with in situ observations are available.	8
5.1	Comparisons of normalised SSM between in situ observations and products; SM-DAS-2 (ECM), ASCAT (ASC) and SMOS (SMO) for 2010. Mean correlation, bias (in situ minus products) and root mean square difference (RMSD) are given for each network and for each product. Scores are presented for significant correlations with p-values ≤ 0.05	18
5.2	Correlations between in situ SSM and each product; SM-DAS-2 (ECM), ASCAT (ASC) and SMOS (SMO) for 2010. For each network, number of significant correlation values (p-value < 0.05) between in situ SSM and each product are ranked as; Inadequate ($R < 0.2$), Poor ($0.2 < R < 0.5$), Fair ($0.5 < R < 0.7$), Good ($R > 0.7$).	22
5.3	Comparisons between in situ SSM and the three products; SM-DAS-2 (ECM), ASCAT (ASC) and SMOS (SMO) SSM anomaly time-series for 2010. Mean correlation, bias (in situ minus analyses) and root mean square difference (RMSD) are given for each network and for each product. Scores are presented for significant correlation values with p-values ≤ 0.05 . Four periods are distinguished: (i) winter, (ii) spring, (iii) summer and (iv) autumn.	24
5.4	Comparisons between in situ SSM observations and products; SM-DAS-2 (ECM), ASCAT (ASC) and SMOS (SMO) for 2010. For normalised and anomaly time-series, mean correlation, bias (in situ minus analyses) and root mean square difference (RMSD) are given for each network and for each product. Scores are presented for stations presenting significant correlation levels (p-values ≤ 0.05) for all the three products. 168 and 165 stations for normalised and anomaly time-series, respectively, are available in this configuration.	26
6.1	Regional scale statistics obtained for 2010 for the products comparison by pair. Regions are defined as shown in Figure 6.7.	36

List of Acronyms

AMSR-E	Advanced Microwave Scanning Radiometer on EOS
ASC	ASCAT
ASCAT	Advanced SCATterometers
CESBIO	Centre d'Etude Spatiale de la BIOSphère
DOY	Day Of Year
ECMWF	European Centre for Medium-Range Weather Forecasts
ECM	ECMWF
EKF	Extended Kalman Filter
ERS	European Remote Sensing
EUMETSAT	European Organisation for the Exploitation of Meteorological Satellites
H-SAF	Hydrology and Water Management
IFS	Integrated Forecast System
IPF	Institute of Photogrammetry and Remote Sensing
ITCZ	InterTropical Convergence Zone
ISMN	International Soil Moisture Network
NASA	National Aeronautics and Space Administration
RMSD	Root Mean Square Difference
SM	Soil Moisture
SMAP	Soil Moisture Active and Passive
SSM/I	Special Sensor Microwave Imager
SMMR	Scanning Multichannel Microwave Radiometer
SMOS	Soil Moisture and Ocean Salinity
SMO	SMOS
TMI	TRMM Microwave Imager
TRMM	Tropical Rainfall Measuring Mission
TUW	Technische Universitaet Wien
ZAMG	Central Institute of Meteorology and Geodynamics

Chapter 1

Introduction

Soil moisture plays a fundamental role in the partitioning of mass and energy fluxes between the hydrosphere, the biosphere and the atmosphere, as it controls both evaporation and transpiration fluxes from bare soil and vegetated areas, respectively. Many applications require global or continental scale soil moisture, to be used as realistic initial states for the soil moisture variables, from forecasts of weather and seasonal climate variations to models of plant growth and carbon fluxes.

A number of studies have been conducted to obtain soil moisture estimates from spaceborne microwave instruments (Wagner et al. 1999; Kerr 2007; Kerr et al. 2010; Njoku et al. 2003). Indeed, quantitative information about the water content of a shallow near surface layer can be obtained from spaceborne microwave instruments (Schmugge 1983a), particularly in the low-frequency microwave region from 1 to 10 GHz. While it was shown that surface soil moisture (SSM) influences the microwave emission of vegetated surfaces from L-band to K-band (1.42-23.8 GHz, (Calvet et al. 1999)), L-band is the optimal wavelength range to observe soil moisture (Wigneron et al. 1995). Higher frequencies are more significantly affected by perturbing factors such as atmospheric effects and vegetation cover (Schmugge 1983a; Kerr 2007). In the last decade microwave remote sensing offered the possibility to obtain soil moisture estimates at global scale with sampling times of few days. However, apart from a few days of L-band radiometric observations on Skylab between June 1973 and January 1974 (Jackson et al. 2004) current or past instruments have been operating at frequencies above 5 GHz.

The Soil Moisture and Ocean Salinity mission (SMOS) is the first dedicated soil moisture mission launched in November 2009 (Kerr 2007; Kerr et al. 2010). It consists of a spaceborne L-band (1.42 GHz, 21 cm) interferometric radiometer able to provide global SSM estimates at a spatial resolution of about 40 km, with a sampling time of 2-3 days. Previous spaceborne microwave radiometers were the Scanning Multichannel Microwave Radiometer (SMMR) which operated on Nimbus-7 between 1978 and 1987 (6.6 GHz and above), followed by the Special Sensor Microwave Imager (SSM/I starting in 1987 at 19 GHz and above) and the TRMM Microwave Imager (TMI) on the Tropical Rainfall Measuring Mission (TRMM) satellite (1997, at 10.7 GHz and above). The Advanced Microwave Scanning Radiometer for the Earth Observing System (AMSR-E on the Aqua satellite from 6.9 to 89.0 GHz), Windsat (from 6.8 to 37 GHz) and the scatterometer on board the European Remote Sensing Satellite (ERS-1&2, 5.3 GHz) are operating closer

to the L-band.

A review of these different active and passive microwave products can be found in (Rüdiger et al. 2009; Gruhier et al. 2010). Another sensor, the Advanced Scatterometer ASCAT onboard METOP-A (launched 2006), produces SSM estimates with a spatial resolution of 50 km and 25 km (resampled to 25 km and 12.5 km grids in the swath geometry). It is the first sensing satellite to provide SSM product in operation and in Near Real Time (NRT). ASCAT is a C-band radar operating at 5.255 GHz (Wagner et al. 2007; Bartalis et al. 2007b; Bartalis et al. 2007a; Albergel et al. 2009). Those spatial missions, as well as the upcoming SMAP (Soil Moisture Active/Passive) mission programmed by the National Aeronautics and Space administration (NASA) demonstrate the relevance of the retrieval of SSM from space within the scientific community.

As sensors and their retrieval algorithms continue to improve, users trust more and more in remotely sensed products. By developing and applying statistical methods to make use of soil moisture properties, remotely sensed data are used as input or as validation, sometimes both. These applications highlight the need to assess satellite products accuracy at a global level.

This study presents an evaluation of two remotely sensed surface soil moisture data sets, ASCAT and SMOS using in situ observations from more than 200 stations across the world (Australia, Africa, America and Europe) for the 2010 period. Along with those data sets, SM-DAS-2 soil moisture analysis from ECMWF/H-SAF is evaluated. The latter relies on an advanced surface data assimilation system an Extended Kalman filter, (Drusch et al. 2009; de Rosnay et al. 2011) used to optimally combine conventional observations with satellite data sensitive to surface variables such as soil moisture from ASCAT. In addition they are compared at global scale and regional scale.

In chapter 2, The three SSM products used in this study, ASCAT and SMOS from remote sensing, ECMWF analysis (SM-DAS-2) and in situ data are described. In chapter 3, the in-situ observation used for local scale evaluation are presented. In chapter 4, the products harmonisation is detailed and the metrics are defined. Chapter 5 provided local scale evaluation results and chapter 6 presents global and regional scale comparison. Section 7 concludes.

Chapter 2

Surface soil moisture products

2.1 SMOS

The SMOS system is a microwave imaging radiometer with aperture synthesis collecting top of atmosphere full polarized radiances coming from the scene viewed by SMOS antennas through their power patterns. It is a Y-shaped instrument where 69 elementary antennas regularly spaced along the arms provide at each integrations step, a full image (circa 1000x1200 km), at either 2 polarisations or full polarisation, of the Earth's surface (Kerr 2007; Kerr et al. 2010). Spatial resolution is about 40 km and the globe is fully imaged at least twice every three days (ascending and descending orbits). Any points at the surface are viewed frequently at different angles and polarisations. The angular information is used to separate the different contributions (soil-vegetation) to the signal (Wigneron et al. 2000). The signal measured at satellite level is a brightness temperature (TB) consisting of four main contributions: (i) the up-welling atmospheric emission, (ii) the Earth's surface emission, attenuated by the atmosphere, (iii) the atmospheric down-welling atmospheric emission reflected at the surface and attenuated along the upward path by the atmosphere; and (iv) the cosmic background emission attenuated by the atmosphere, reflected at the surface and attenuated again along the upward path by the atmosphere. At L-band, up to the first 5 cm of soil are sampled. The principle of the SMOS level 2 product is to find the best-suited set of SSM and vegetation characteristics which minimizing a cost function; the differences between modelled direct and measured angular TB data (Waldteufel and Vergely 2003; Kerr et al. 2007). The resulting SMOS level 2 product is complemented by a Data Quality index (DQX), an index related to the quality of the retrieved parameter. It takes into account the error in the parameter retrieval as well as the L1C TB accuracy. It is provided in the parameter units (volumetric soil moisture units, usually between 0 and 0.1 for soil moisture for instance). The SMOS level 2 product used in this study was provided by CESBIO (Centre d'Etudes Spatiale de la Biosphere), as for the other products, the year 2010 is considered.

2.2 ASCAT SM-OBS-1 product

Like its predecessor ERS-1&2 scatterometers, ASCAT is a real-aperture radar instrument measuring radar backscatter with very good radiometric accuracy and stability (Bartalis et al. 2007b). ASCAT uses a VV polarization in the C-band (5.255 GHz) and observes the surface of the Earth with a spatial resolution of circa 50 km or 25 km. Measurements occur on both sides of the subsatellite track, thus two 550 km wide swaths of data are produced. Because ASCAT operates continuously and it has a double swath, more than twice of the ERS scatterometer coverage is provided.

On both sides of METOP-A, ASCAT produces a triplet of backscattering coefficients (σ_0) from the three different antenna beams. A σ_0 measurement is the result of averaging several radar echoes. Backscatter is registered at various incidence angles and it is possible to determine the yearly cycle of the backscatter-incidence angle relationship. This is an essential prerequisite for correcting seasonal vegetation effects (Bartalis et al. 2007b; Bartalis et al. 2007a). The spatial and temporal behaviour of the scatterometer is affected by land cover and vegetation phenology. It was demonstrated that by using a time series-based approach for the soil moisture retrieval, the influence of the vegetation could be minimized (Wagner et al. 1999). In order to retrieve surface soil moisture from ERS scatterometer, (Wagner et al. 1999), proposed a time-series based change-detection approach where the backscattering coefficient extrapolated to a reference angle at 40° is scaled using the lowest and highest backscattering coefficient values measured over a long period. The theoretical background of this method is described in detail in (Wagner et al. 1999).

ASCAT provides a relative measure of the soil moisture content in the first few centimetres of the soil which are sensed by C-band microwaves. According to (Schmugge 1983b), the depth of this layer is about 0.5 to 2 cm. Thus, ASCAT measurement represents the degree of saturation of the topmost soil layer and is given in percent ranging from 0 (dry) to 100 % (wet). This measure is complemented by an error estimate, derived by error propagation of the backscatter noise (ranging from 0 to 100 %, covering instrument noise, speckle and azimuthal effects). Even if satellite sensors sample the very first centimetres of soil, their derived surface soil moisture related information can be propagated in deeper layers using techniques such as the EKF (Walker et al. 2001; Sabater et al. 2008).

A first ASCAT soil moisture data set was evaluated over southwestern France (Albergel et al. 2009) with encouraging results. This data set used change detection parameters derived from the analysis of multi annual backscatter time series using ERS data over a 15-yr long period. (Brocca et al. 2010a) then used a new ASCAT data set developed by deriving the change detection model parameter from the analysis of ASCAT time series of the 2007-2008 period (Wagner et al. 2010; Hahn and Wagner 2011). This new data set is able to provide reliable soil moisture estimates across different test sites in Europe, with reduced noise with respect to the initial ASCAT soil moisture product. Other findings of evaluating ASCAT-derived soil moisture over Europe, as well as its use in Numerical Weather Prediction (NWP) model and hydrological models through data assimilation can be found in (Brocca et al. 2010b; Mahfouf 2010; Draper et al. 2011).

2.3 SM-DAS-2

The IFS (Integrated Forecast System) Land Surface Data assimilation System used to produce SM-DAS-2 are 36r1, 36r3 and 36r4 (more information: <http://www.ecmwf.int/research/ifsdocs/>). SM-DAS-2 is produced by ECMWF for the H-SAF and it is available at a spatial resolution of about 25 km (Gaussian reduced grid at T799). The generation of SM-DAS-2 relies on an advanced surface data assimilation system used to optimally combine conventional observations with satellite measurements. It is based on an Extended Kalman Filter (EKF), as described by (Drusch et al. 2009; de Rosnay et al. 2011). In its current configuration, the EKF soil moisture analysis uses the two-metre air temperature and two-metre air relative humidity (T2m and RH2m, respectively) screen level parameters as well as ASCAT surface soil moisture as input (de Rosnay et al. 2011). The land surface model used is HTESSEL (van den Hurk and Viterbo 2003; Balsamo et al. 2009), a multilayer model where the soil is discretized in four layers of 0.07, 0.28, 0.72, and 2.89 m depths (from top to bottom). The surface analysis is independent from the 4D-VAR atmospheric analysis. SM-DAS-2 analysis is available daily at 00:00 UTC. SM-DAS-2 is not the first attempt to use satellite derived SSM at ECMWF. (Scipal et al. 2008), examined the potential of ASCAT SSM from its predecessors, ERS-1&2. A nudging scheme similar to the one in (Dharssi et al. 2011) was used to assimilate those data, authors found an increase in correlation and a decrease in root mean square difference when comparing the resulting soil moisture analysis to in situ data of the Oklahoma Mesonet.

Chapter 3

In situ soil moisture observations

In situ soil moisture observations are necessary to evaluate both remotely sensed and modelled soil moisture. In the recent years huge efforts were made to make available such observations in contrasting biomes and climate conditions. Some of them are now freely available on the Internet such as data from NCRS-SCAN (Natural Resources Conservation Service - Soil Climate Analysis Network) in the United States ((Schaefer and Paetzold 2000), <http://www.wcc.nrcs.usda.gov/scan/>) or the OZNET hydrological monitoring network in Australia ((Young et al. 2008), <http://www.oznet.org.au/>). The International Soil Moisture Network (ISMN, (Dorigo et al. 2011), <http://www.ipf.tuwien.ac.at/insitu/>), a new data hosting centre where globally available ground based soil moisture measurements are collected, harmonized and made available to users, is also a clear evidence of how relevant the availability of such data is for the scientific community. Other data sets used in this study were obtained by request from the concerned organisations such as Météo-France for the SMOSMANIA and SWATMEX data in southwestern France and the LTHE for the AMMA data in western Africa. The different soil moisture data sets used in this study are described in Table 3.1 and presented in Figure 3.1. For each station available, a quality check of the data was performed and suspicious data were eliminated. 229 of 252 available stations were retained for this study, so 23 of them were rejected from this first visual quality check.

3.1 NCRS-SCAN

The SCAN network (<http://www.wcc.nrcs.usda.gov/scan/>) is a comprehensive, nationwide soil moisture and climate information system designed to provide data to support natural resource assessments and conservation activities. Administered by the United States Department (USDA) of Agriculture Natural Resources Conservation Service (NRCS) through the National Water and Climate Center (NWCC), in cooperation with the NRCS National Soil Survey Centre, the system focuses on agricultural areas of the U.S. monitoring soil temperature and soil moisture content at several depths, soil water level, air temperature, relative humidity, solar radiation, wind, precipitation, barometric pressure, among others. SCAN data are used for various studies from global climate modelling to agricultural studies. Data are collected by a dielectric constant measuring device, typical measurements at 2 inches (about 5 cm) are used. In this study, all the stations of the

Soil Moisture data set	Type	Soil layer depth (cm)	Spatial resolution	Number of stations
ECMWF SM-DAS-2	NWP analysis	0-7	25 km (T799)	Global product
ASCAT	Remotely sensed product	C-band, 0.5-2	25 km	Global product
SMOS level 2 product	Remotely sensed product	L-band, 5	40 km	Global product
SMOSMANIA (France)	In situ observations	5, 10, 20, 30	Local scale	12 stations
SWATMEX (France)	In situ observations	5, 10, 20, 30	Local scale	9 stations
OZNET (Australia)	In situ observations	0-5 or 0-8 and 0-30	Local scale	38 stations
NCRS-SCAN (US)	In situ observations	5, 20	Local scale	154 stations
AMMA (West Africa)	In situ observations	5	Local scale	10 stations
REMEDHUS (Spain)	In situ observations	5	Local scale	21 stations
UMSUOL (Italy)	In situ observations	10	Local scale	1 station
UDC-SMOS (Germany)	In situ observations	5	Local scale	7 stations

Table 3.1: Presentation of the different soil moisture data sets used in this study. NWP stands for numerical weather prediction. 252 stations with in situ observations are available.

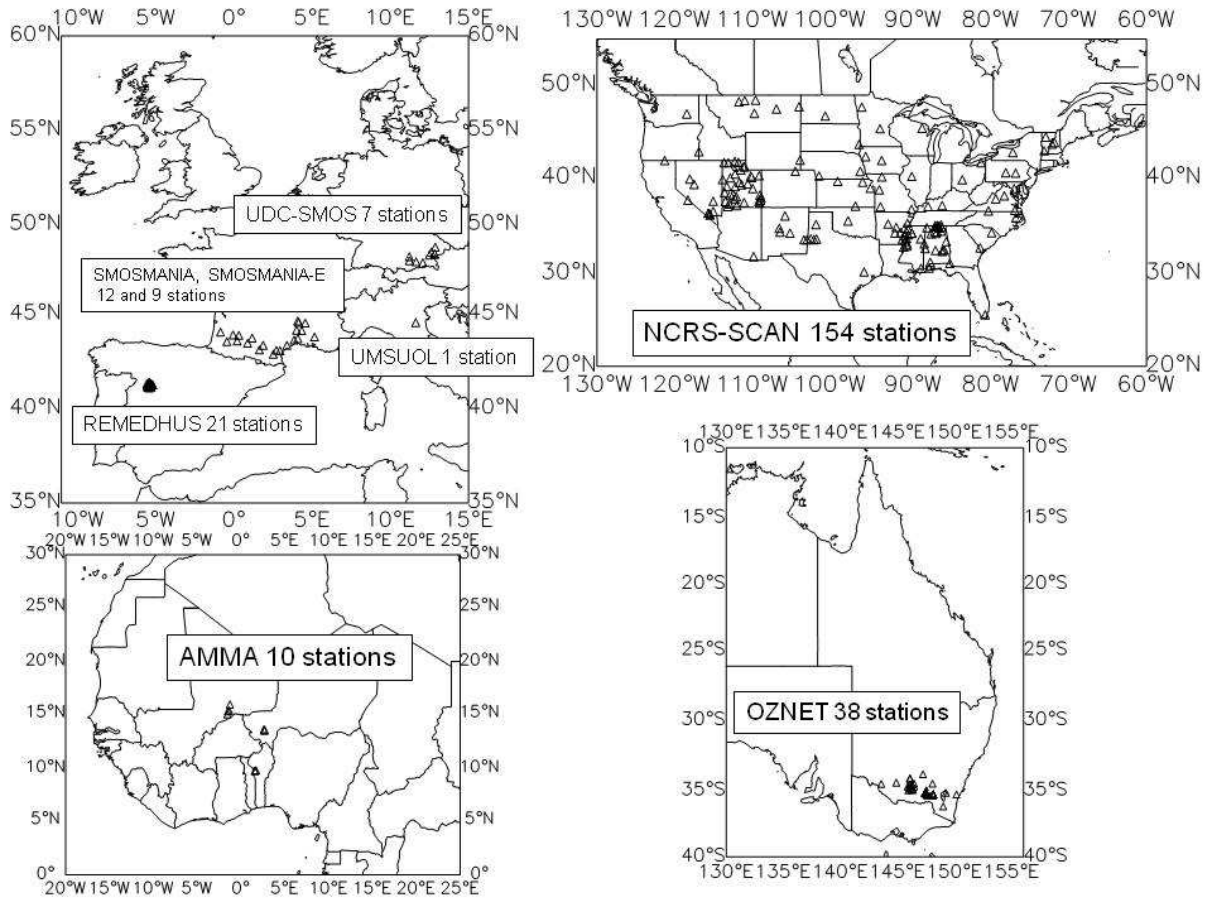


Figure 3.1: Location of the different in situ soil moisture stations used in this study, 38 in Australia (OZNET network), 154 within the United States (NCRS-SCAN network), 10 in Western Africa (AMMA network), 21 in southwestern France (SMOSMANIA and SWATMEX networks), 7 in Germany (UDC-SMOS network) and 1 in Italy (UMSUOL).

NCRS-SCAN network presenting data in 2010 network are used (154 stations).

3.2 SMOSMANIA and SWATMEX

The SMOSMANIA project is a long-term data acquisition effort of soil moisture observations in Southwestern France (Albergel et al. 2008)(Calvet et al., 2007). Soil moisture profile measurements at 12 automated weather stations of Météo-France from the RADOME network (Réseau d'Acquisition de Données d'Observations Météorologiques Etendu), have been obtained since January 2007 at four different depths (5, 10, 20 and 30 cm) with a 12 minutes time step. Stations span from the Mediterranean Sea to the Atlantic Ocean. The soil moisture measurements are in units of $m^3 m^{-3}$, they are derived from capacitance probes: ThetaProbe ML2X of Delta-T Devices. ThetaProbes provide a signal in units of volt and their variations are virtually proportional to changes in the soil moisture content over a large dynamic range. In order to convert the voltage signal into a volumetric soil moisture content, site-specific calibration curves were developed using in situ gravimetric soil samples, for each station, and each depth (i.e., 48 calibrations curves). In January 2009, 9 additional RADOME stations were equipped with ThetaProbe in south and south eastern France. They form the SWATMEX (Soil Water and Temperature in Mediterranean EXPeriment) network. Data at 5 cm over the year 2010 are used in this study.

3.3 AMMA

In the framework of AMMA (African Monsoon Multidisciplinary Analysis) project dedicated to improve our understanding and our modelling capabilities of the effect of land surface processes on monsoon intensity, variability and predictability (Redelsperger et al. 2006), West Africa has been extensively instrumented. Three meso-scale sites were implemented in Mali (de Rosnay et al. 2009), Niger (Pellarin et al. 2009a) and Benin (Pellarin et al. 2009b), providing information along the North-South gradient between Sahelian and Soudanian regions. Soil moisture and other data are collected at different stations within the three meso-scale sites. The same installation protocol is used for all the soil moisture stations, where Time Domain Reflectometry sensors are used (Campbell CS616). When they were not suitable (e.g. due to soil texture), Delta-T Theta Probes were used. Three stations in Niger and 3 in Benin are used in this study. Data are collected at 5 cm.

3.4 OZNET

The OZNET network ((Young et al. 2008), <http://www.oznet.org.au>) is located within the Murrumbidgee experimental catchment in southern New South Wales, Australia. Each soil moisture site of the Murrumbidgee monitoring network (38) measures the soil moisture between 0-5 cm with soil dielectric sensor (Stevens Hydraprobe®) or 0-8 cm, 0-30 cm, 30-60 cm and 60-90 cm with water content reflectometers (Campbell Scientific). Hydraprobes are soil dielectric sensor operating at 50 MHz. At each measurement point, a

volumetric soil moisture value is inferred from the real component of the measured relative dielectric constant and the conductivity from the imaginary component. Reflectometers measure the travel time of an output pulse to estimate changes in the bulk soil dielectric constant. Measurement is converted to volumetric water content with a calibration equation parameterised with soil type and soil temperature. As sensor response to soil moisture may vary with soil characteristics such as salinity, density, soil type and temperature, soil moisture sensor calibration was undertaken using both laboratory and field measurements. Reflectometer measurements were compared with both field gravimetric samples and Time-Domain Reflectometry (TDR) measurements. TDR measurements are based on the relationship between the dielectric properties of soils and their moisture content, also. Surface soil moisture observations are used in this study (either 0-5 cm or 0-8 cm).

3.5 ISMN soil moisture: REMEDHUS, UDC-SMOS and UMSUOL

Several stations from the 3 different networks were obtained through the ISMN website, 21 from the REMEDHUS network in Spain, 9 from the UDC-SMOS network in Germany and one from UMSUOL in Italy. REMEDHUS is located in the central sector of the Duero basin. Each station has been equipped with capacitance probes (HydraProbes, Stevens) installed horizontally at a depth of 5 cm. Analysis of soil samples were carried out to verify the capacitance probes and to assess soil properties at each station (Martínez-Fernández and Ceballos 2005). Data from UDC-SMOS in Germany (Loew et al. 2010) near the city of Munich are collected with TDR (IMKO-TDR) at 5 cm. This soil moisture network is run in cooperation with the Bavarian State Research Center for Agriculture and is carried out as part of the project SMOSHYD (FKZ 50EE0731) funded by the German Aerospace Centre (DLR). Finally, the San Pietro Capofiume station (Brocca et al. 2011) belonging to the UMSUOL network located in northern Italy it used. It was installed by the Service of Hydrology, Meteorology and Climate of the regional Agency for Environmental Protection in Emilia-Romagna (ARPA-SIMC, <http://www.arpa.emr.it/sim/>). Data are collected at 10 cm with TDR (TDR100, Campbell Scientific Inc).

Chapter 4

Methods

4.1 Harmonisation of the data and metrics used for the local comparison

ASCAT SSM estimates represent a relative measure of the soil moisture in the first centimetres of soil and it is given in percent, SM-DAS-2 is an index (between [0,1]), SMOS and in situ data are in m^3m^{-3} . Hence, to enable a fair product comparison, all soil moisture data sets (in situ, remotely sensed and modelled) are scaled between [0,1] using their own maximum and minimum values over the year 2010. The nearest neighbour technique is used to make a correspondence between SM-DAS-2, ASCAT, SMOS and in situ SSM. Time steps for in situ data range from 12-min (e.g. SMOSMANIA, SWATMEX) to 1 hour (e.g. NCRS-SCAN). SM-DAS-2, ASCAT, SMOS and in situ SSM are available at different time of the day, each of them is collocated in time with ground observations. For all stations, correlations (R, Eq. 4.1), bias (in situ minus analysis), root mean square difference (RMSD, Eq. 4.2) and p-value (a measure of the correlation significance) are calculated for the whole 2010 year. The latter indicates the significance of the test, the 95% confidence interval is used in this study (Rüdiger et al. 2009; Albergel et al. 2009); configurations where the p-value is below 0.05 (i.e. the correlation is not a coincidence) are retained. In situ data contain errors (instrumental and representativeness), so they are not considered as 'true' soil moisture. This is underlined here by using the RMS Difference terminology instead of RMS Error.

$$R = \sqrt{1 - \frac{(SSM_{product} - SSM_{insitu})^2}{(SSM_{product} + SSM_{insitu})^2}} \quad (4.1)$$

$$RMSD = \sqrt{(SSM_{product} - SSM_{insitu})^2} \quad (4.2)$$

4.2 Harmonisation of the data for the global comparison

SM-DAS-2, ASCAT and SMOS were produced on three different grids and with three different formats. For global scale comparison the three products were regrided, using

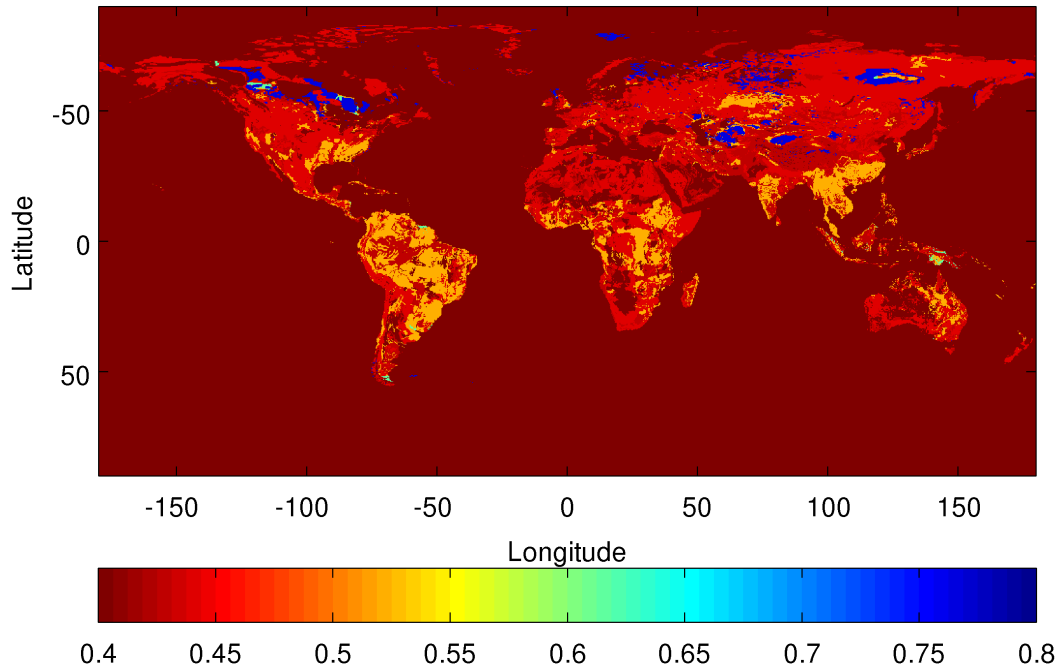


Figure 4.1: Global map of volumetric soil moisture at saturation (in m^3m^{-3}), obtained from the dominant type of global soil texture map derived from Food and Agriculture Organization digital soil map. This information is used in this study to convert SM-DAS-2 and ASCAT into volumetric soil moisture products.

a bi-linear interpolation procedure, on the same regular latitude-longitude grid at a 0.25 degrees resolution. The interpolated products were then save in a common GRIB format and archived at ECMWF on the ECFS (ECMWF File Storage system).

In addition, the products were converted to use a common soil moisture unit that allows quantitative comparison. In contrast to local scale comparisons, based on soil moisture index as described in the previous section, global scale comparison considers the three products expressed in volumetric soil moisture. So, the SMOS product is kept with its original volumetric unit, while ASCAT and SM-DAS-2 are converted to volumetric unit. The conversion factor used for this study is the global scale map of volumetric soil moisture at saturation obtained from the dominant type of global soil texture map derived from Food and Agriculture Organization digital soil map (Figure 4.1). For each date and each grid point, ASCAT and SM-DAS index are multiplied by the collocated volumetric soil moisture at saturation. Global comparison shown in Chapter 6 are based on the interpolated products expressed in volumetric units (m^3m^{-3}).

4.3 Anomalies

In order to avoid seasonal effects, anomaly time-series are also calculated. The difference to the mean is calculated for a sliding window of five weeks (if there are at least five measurements in this period), and the difference is scaled to the standard deviation. For each SSM estimate at day (i), a period F is defined, with $F=[i-17, i+17]$ (corresponding to a 5-week window). If at least five measurements are available in this period of time, the average SSM value and the standard deviation are calculated. The Anomaly (Ano), dimensionless is then given by:

$$Ano(i) = \frac{SSM(i) - \overline{SSM(F)}}{stdev(SSM(F))} \quad (4.3)$$

The same equation is used to compute in situ anomaly time-series which can be compared with the ASCAT, SMOS and ECMWF soil moisture anomaly time-series.

4.4 Additional metrics for Taylor diagram

Additionally, the normalised standard deviation (SDV) and the centred root mean square difference between analysis and in situ patterns, normalised by the in situ standard deviations (E) are computed. SDV is the ratio between SSM product and in situ standard deviations; it gives the relative amplitude whilst E quantifies errors in the pattern variations. It does not include any information on biases since means of the fields are subtracted before computing second order errors. SDV and E are expressed by Eq. 4.4 and Eq. 4.5, respectively:

$$SDV = \sigma_{SSM_{product}} / \sigma_{SSM_{insitu}} \quad (4.4)$$

$$E^2 = (RMSD^2 - Bias^2) / \sigma_{insitu}^2 \quad (4.5)$$

R , SDV and E are complementary but not independent as they are related by Eq. 4.6 (Taylor 2001):

$$E^2 = SDV^2 + 1 - 2SDV * R \quad (4.6)$$

Taylor diagrams are used to represent these three different statistics on two dimensional plots. The normalized standard deviation is displayed as a radial distance and the correlation with in situ data as an angle in the polar plot. In situ data are represented by a point located on the x axis at $R=1$ and $SDV=1$. The distance to this point represents the centred normalized RMS difference (E) between the analysis and in situ patterns.

4.5 Hovmöller plots

Hovmöller plots show time-latitude variations for a fixed averaged longitudinal area. They are very usefull to spot seasonal scale latitudinal variations of climate related variables. They are used in this report to compare SMOS, ASCAT and SM-DAS-2 at global scale (Chapter 6).

Chapter 5

Local comparison

5.1 Comparison of the normalised times series

The statistical scores for the comparison between SM-DAS-2, ASCAT, SMOS (referred as ECM, ASC and SMO in the following of the paper) and in situ SSM are presented in Table 5.1. Only the configurations associated to significant correlation values (p-value ≤ 0.05) are considered leading to 219, 208 and 180 stations available for ECM, ASC and SMO, respectively. In average, for all the stations, correlation values are 0.70, 0.53 and 0.54 for ECM, ASC and SMO. SMOSMANIA in southwestern France and OZNET in Australia present the best correlation values for ECM (0.83 and 0.82 in average) while AMMA in western Africa presents a correlation value average of 0.45.

Considering the use of ASC in ECM analysis, previous studies (de Rosnay et al. 2011; Albergel et al. 2010) indicated that ASC assimilation has a neutral impact on soil moisture analyses. Its use requires that ASC data are matched to ECMWF IFS soil moisture using a bias correction method; a Cumulative Distribution Function (CDF) matching as described in (Scipal et al. 2008). Coming improvement in the ASC soil moisture products and in bias correction at ECMWF are expected to enhance the impact of using ASC soil moisture data.

For ASC, best correlation values are obtained with OZNET (0.80) and poor values are found in Germany (UDC-SMOS) and southeastern France (SWATMEX), 0.30 and 0.33. Several authors (Albergel et al. 2010; Brocca et al. 2010b; Draper et al. 2011) found higher level of correlations, but considered reprocessed ASC data set. In this study, near real time (NRT) data from EUMETSAT are used, as in (Albergel et al. 2009), who found similar correlations levels over the SMOSMANIA network for a 6 month period in 2007 (0.58 against 0.52 here for a one year period; 2010). This ASC data set was retained for this study as it is the official operational ASC product available in NRT via EUMETSAT and disseminated to NWP community.

Radio frequency interference (RFI) disturbs the natural microwave emission observed by SMO, hence the soil moisture retrieval. Their impact on Western Europe (e.g. in southwestern France, (Zribi et al. 2011; Albergel et al. 2011)) as well as over the United State (Parinussa et al. 2011) are known. The OZNET network in Australia, which presents the best correlation values for SMO, does not seem to be affected by RFI with an aver-

Soil Moisture data set	Number of stations with p-values<0.05			Correlation [-]			Bias [-]			RMSD [-]		
	ECM	ASC	SMO	ECM	ASC	SMO	ECM	ASC	SMO	ECM	ASC	SMO
SMOSMANIA (France)	11	11	10	0.83	0.52	0.44	-0.178	-0.037	0.124	0.242	0.254	0.273
SWATMEX (France)	9	8	6	0.79	0.33	0.40	-0.274	-0.140	0.101	0.345	0.284	0.235
OZNET (Australia)	36	34	30	0.82	0.80	0.74	-0.013	-0.021	0.195	0.178	0.184	0.255
NCRS-SCAN (US)	131	125	106	0.65	0.48	0.51	-0.022	-0.078	0.095	0.233	0.266	0.232
AMMA (West Africa)	5	6	6	0.45	0.55	0.42	-0.074	-0.179	0.079	0.531	0.407	0.316
REMEDHUS (Spain)	17	17	17	0.79	0.57	0.52	-0.118	-0.088	0.128	0.243	0.245	0.232
UMSUOL (Italy)	1	1	1	0.76	0.39	0.54	-0.176	0.077	0.167	0.233	0.237	0.240
UDC-SMOS (Germany)	9	6	4	0.59	0.30	0.29	-0.061	0.052	0.267	0.198	0.267	0.344
All stations	219	208	180	0.70	0.53	0.54	-0.050	-0.068	0.120	0.235	0.255	0.243

Table 5.1: Comparisons of normalised SSM between in situ observations and products; SM-DAS-2 (ECM), ASCAT (ASC) and SMOS (SMO) for 2010. Mean correlation, bias (in situ minus products) and root mean square difference (RMSD) are given for each network and for each product. Scores are presented for significant correlations with p-values ≤ 0.05 .

aged correlation value of 0.74. In addition to the RFI issue, ASC and SMO signals are influenced by the vegetation. A reduced sensitivity to soil moisture is to be expected over dense vegetation canopies. A possible explanation of the good scores obtained with SMO and ASC over the OZNET network could be the presence of a significant fraction of bare soil and/or of dry vegetation, caused by the crop rotation practice; land use in the Murrumbidgee catchment is predominantly agricultural (Young et al. 2008). Moreover, if the indication given by the dqx can only be considered as indicative so far, (according to the guide of Release of SMOS level 2 products to Cal/Val teams) several tests with various dqx values permit to set a threshold of 0.045 m³m⁻³ allowing an increase in the correlation levels for SMOS. Scores obtained in this study with SMO data consider this threshold.

Biases are in average of -0.050, -0.068 and 0.120 (in situ minus SSM products, dimensionless) for ECM, ASC and SMO, respectively. Negative biases are found with ECM, it concerns all networks used in this study. On the contrary, SMO systematically presents positive averaged biases. Averaged RMSD are 0.235, 0.255 and 0.243 for ECM, ASC and SMO, respectively. The RMSD represents the relative error of the soil moisture dynamical range. The average dynamic range observed for each network, associated to the average RMSD values of each network permits to give an estimate of the average error in volumetric soil moisture; about 0.07 m³m⁻³, 0.08 m³m⁻³ and 0.08 m³m⁻³ for ECM, ASC and SMO, respectively.

Figure 5.1 presents three Taylor diagrams illustrating the statistics of the comparison between ECM, ASC and SMO and in situ data. They correspond to three networks used in this study, REMEDHUS in Spain, OZNET in Australia and SMOSMANIA in France. These diagrams underline the good range of correlation obtained for ECM with most of the values between 0.70 and 0.90 while ASC and SMO present lower values. It is particularly clear for SMOSMANIA (Figure 5.1C), moreover, for this network, symbols representing ASC and SMO are most of the time below the SDV value of 1 (red dashed line on Figure 5.2); as SDV is the ratio between analysed and in situ standard deviation (see Eq.4) it indicates that the variability of the in situ data is higher than the one of ASC and SMO for this group of stations. For the OZNET network (Figure 5.1B) however, the three products present good levels of correlation (most of the time above 0.70). Figure 5.2 presents three Taylor diagrams illustrating the statistics of the comparison between ECM, ASC and SMO and in situ data for the NCRS-SCAN network. Correlation values are better for ECM than for ASC and SMO, which is in line with Table 5.1. SMO presents better correlation values than ASC and a smaller dispersion in term of SDV. However its variability is smaller than in situ data.

Table 5.2 presents for each network and each product the count (in %) of significant R values ranked as: Inadequate ($R < 0.2$), Poor ($0.2 < R < 0.5$), Fair ($0.5 < R < 0.7$) and Good ($R > 0.7$). Considering the NCRS-SCAN network, ECM presents 34% of good, 50% of fair, 14% of poor and only 2% of inadequate R. ASC and SMO present 7% and 17% of good correlations. Figure 5.3 presents correlation values for ECM, ASC and SMO, for the NCRS-SCAN network, values are ranked using the same intervals above-mentioned. For this network, most stations present better correlation values when in situ data are compared to SMO data than with ASC data (57%).

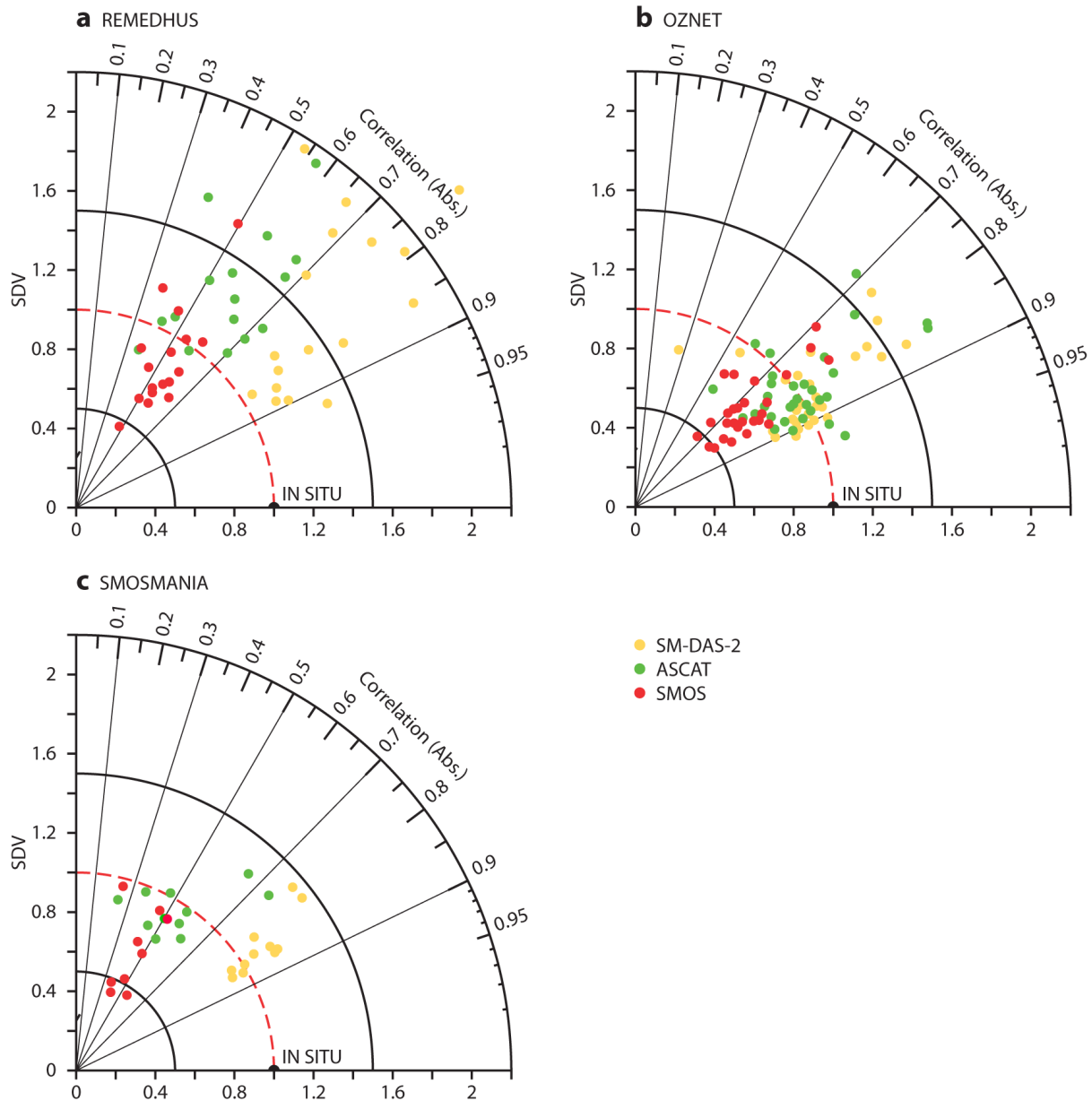


Figure 5.1: Taylor diagram illustrating the statistics of the comparison between SM-DAS-2, ASCAT, SMOS and in situ SSM for a) the REMEDHUS network in Spain, b) the OZNET network in Australia and c) the SMOSMANIA network in France. Yellow circles are for SM-DAS-2, green circles for ASCAT and red circles for SMOS.

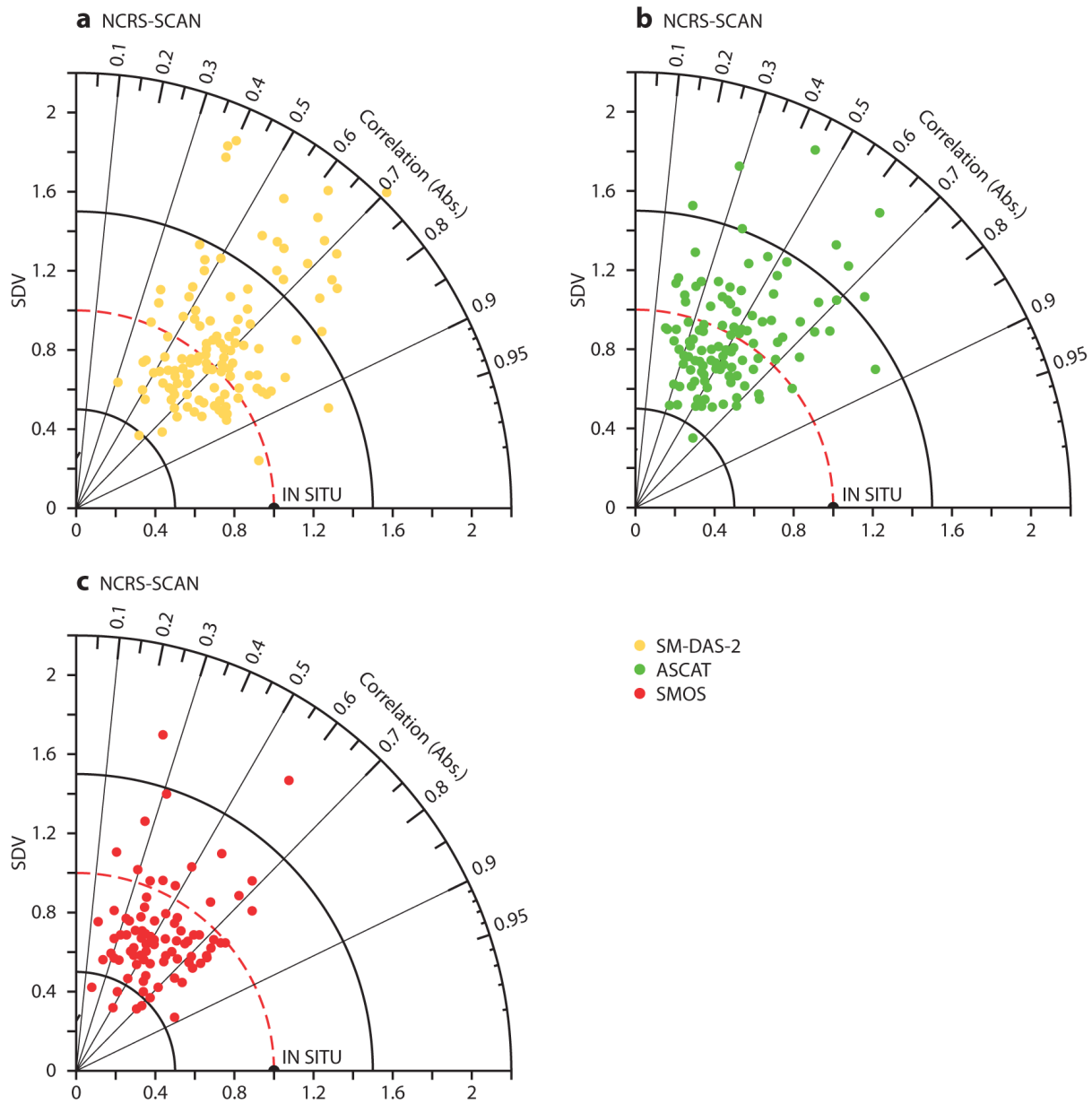


Figure 5.2: Taylor diagram illustrating the statistics of the comparison between a) SM-DAS-2, b) ASCAT, c) SMOS and in situ SSM for the NCRS-SCAN network. Yellow circles are for SM-DAS-2, green circles for ASCAT and red circles for SMOS.

Soil Moisture data set	Inadequate (%) $R < 0.2$			Poor (%) $0.2 < R < 0.5$			Fair (%) $0.5 < R < 0.7$			Good (%) $R > 0.7$		
	ECM	ASC	SMO	ECM	ASC	SMO	ECM	ASC	SMO	ECM	ASC	SMO
SMOSMANIA (France)	0	0	0	0	45	80	0	46	20	100	9	0
SWATMEX (France)	0	25	0	0	50	83	0	25	17	100	0	0
OZNET (Australia)	0	0	0	3	0	0	3	12	20	94	88	80
NCRS-SCAN (US)	2	7	3	14	47	48	50	39	32	34	7	17
AMMA (West Africa)	20	0	0	20	17	83	60	83	17	0	0	0
REMEDHUS (Spain)	0	0	0	0	23	41	18	65	59	82	12	0
UMSUOL (Italy)	0	0	0	0	100	100	0	0	0	100	0	0
UDC-SMOS (Germany)	0	17	0	11	83	100	89	0	0	0	0	0
All stations	1	6	2	10	38	44	37	36	31	52	20	23

Table 5.2: Correlations between in situ SSM and each product; SM-DAS-2 (ECM), ASCAT (ASC) and SMOS (SMO) for 2010. For each network, number of significant correlation values (p -value < 0.05) between in situ SSM and each product are ranked as; Inadequate ($R < 0.2$), Poor ($0.2 < R < 0.5$), Fair ($0.5 < R < 0.7$), Good ($R > 0.7$).

For ECM, more than 80% of good correlation values are found for 5 networks out of 8 (OZNET, REMEDHUS, SMOSMANIA and SWATMEX) and even 100% for 2 (SMOSMANIA and SWATMEX networks). For all the stations, ECM presents 52% of good correlation values, ASC 20% and SMO 23%. Most of the correlations for ECM are above 0.70 while the main parts for ASC and SMO are between 0.2 and 0.5 (38% and 44%, respectively). For the OZNET network (38 stations) most of the correlation values are above 0.70; with 94%, 88% and 80% for ECM, ASC and SMO, respectively.

5.2 Comparison of the anomaly time-series

Results presented above give an overview of the products comparison at the annual scale. They are driven to a large extent by the seasonal cycle. To address the ability of the product to capture the short term scale SSM variations, anomaly time-series were calculated (sect 2.5) and statistics are computed on the anomaly time-series. Only the configurations associated to significant correlation values (p -value > 0.05) are considered, leading to 209, 217 and 178 stations retained for ECM, ASC and SMO respectively. Scores were computed in four different periods in 2010 defined as follows: (i) winter (January, February and December), (ii), spring (March to May), (iii) summer (June to August), (iv) autumn

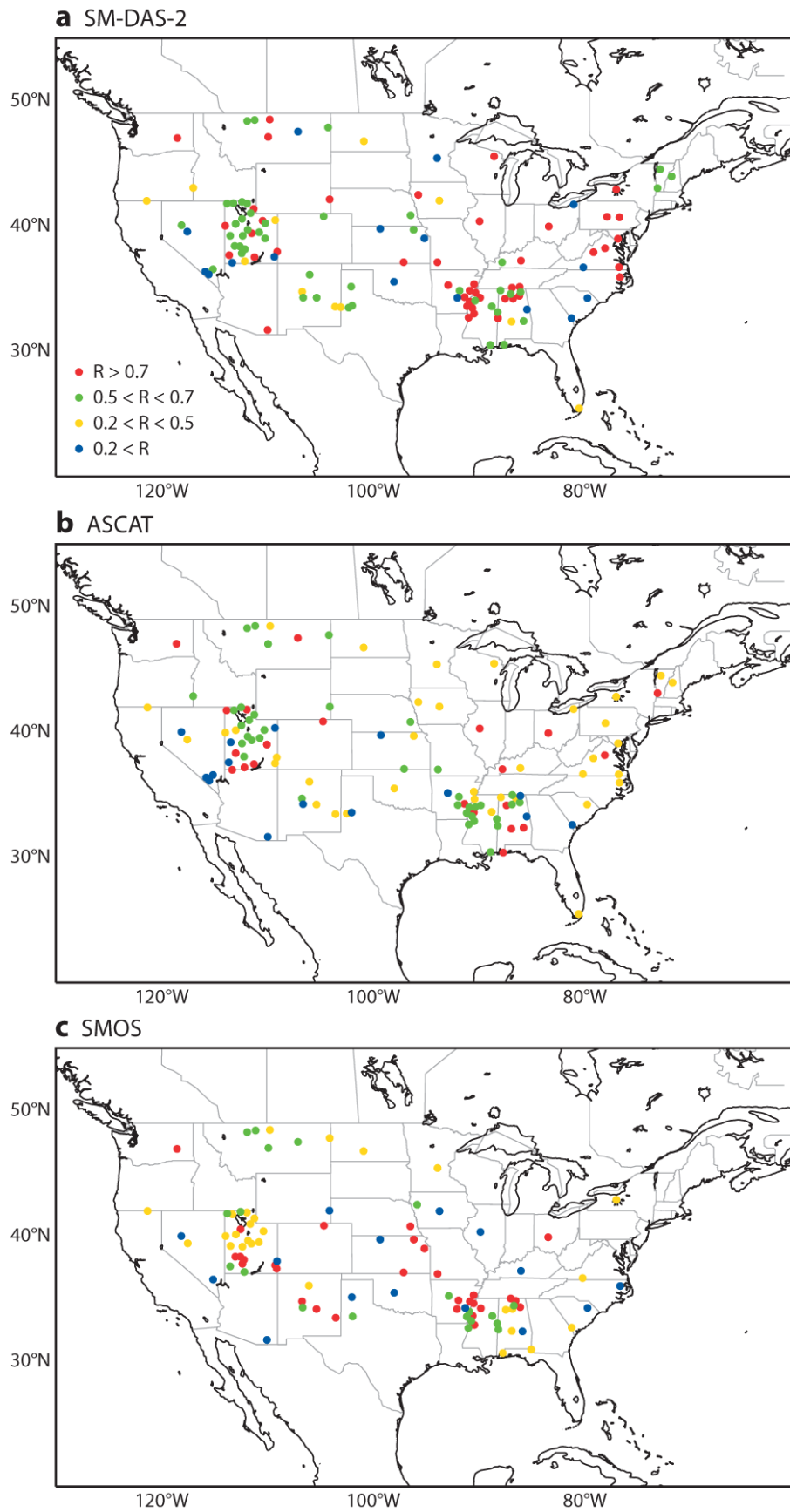


Figure 5.3: Correlation values between in situ SSM and (from top to bottom) ECMWF SM-DAS-2 product, ASCAT and SMOS for the stations of the NCRS-SCAN network.

Season	Correlation [-]			Bias [-]			RMSD [-]		
	ECM	ASC	SMO	ECM	ASC	SMO	ECM	ASC	SMO
Winter	0.70	0.71	0.55	-0.023	0.031	-0.014	0.674	0.686	0.865
Spring	0.65	0.56	0.51	-0.004	0.042	8.10-4	0.766	0.889	0.928
Summer	0.53	0.46	0.46	-0.014	-0.052	3.10-4	0.857	0.964	0.962
Autumn	0.62	0.50	0.45	-0.008	-0.013	-0.017	0.761	0.916	0.967

Table 5.3: Comparisons between in situ SSM and the three products; SM-DAS-2 (ECM), ASCAT (ASC) and SMOS (SMO) SSM anomaly time-series for 2010. Mean correlation, bias (in situ minus analyses) and root mean square difference (RMSD) are given for each network and for each product. Scores are presented for significant correlation values with p-values ≤ 0.05 . Four periods are distinguished: (i) winter, (ii) spring, (iii) summer and (iv) autumn.

(September to November). These periods were used to study the seasonal variation of the scores. The statistical scores for the comparison between ECM, ASC and SMO and in situ SSM anomaly time-series are presented in Table 5.3. On average, for all the stations and considering the two first periods (winter and spring) correlation values are: 0.70 for ECM, 0.71 for ASC and 0.55 for SMO, 0.65 for ECM, 0.56 for ASC and 0.51 for SMO, respectively. However in summer, they are lower, 0.53 for ECM, 0.46 for ASC and 0.46 for SMO. The three products evaluated in this study better capture the soil moisture short term variability in winter and spring than in summer. Correlation values for autumn are 0.62, 0.50 and 0.45 for ECM, ASC and SMO, respectively. Figure 5.4 presents anomaly time series derived from, ECM, ASC, SMO and in situ observations for a randomly chosen station; the Creon d’Armagnac station of the SMOSMANIA network in southwestern France. Most peaks and troughs are well represented for the three soil moisture products. However, in summer ECM (Figure 5.4, top) represents two peaks (first days of June and August) that are not presented in the observations. Representativeness of local rainfall (the main driver of soil moisture temporal pattern) locally observed could induce discrepancies when compared to coarse resolution products, particularly in summer where local storm events may occur in southwestern France. ECM analysis does not assimilate rainfall, the information contained in observations of air temperature and humidity close to the surface as well as ASCAT SSM are used to analyse soil moisture. The use of precipitation data in the analysis is ongoing work at ECMWF; (Lopez 2011) has demonstrated a positive impact on model performance of the direct 4D-Var assimilation of 6-hourly radar and rain-gauge rainfall accumulations. However, additionally to this representativeness issue, the two precipitations events highlighted by Figure 5.4 in ECM are not spotted by the two remotely sensed products which are in line with the observations.

Figure 5.5 presents scatter plots of the three products correlation performances compared by pairs of two. The top panel shows correlation values for the normalised time series and the bottom panel shows the anomaly correlations values. Normalised time-series correlation values scatter plots permit to see that ECM presents better correlation values than ASC and SMO (most of the correlations below the first diagonal), anomaly

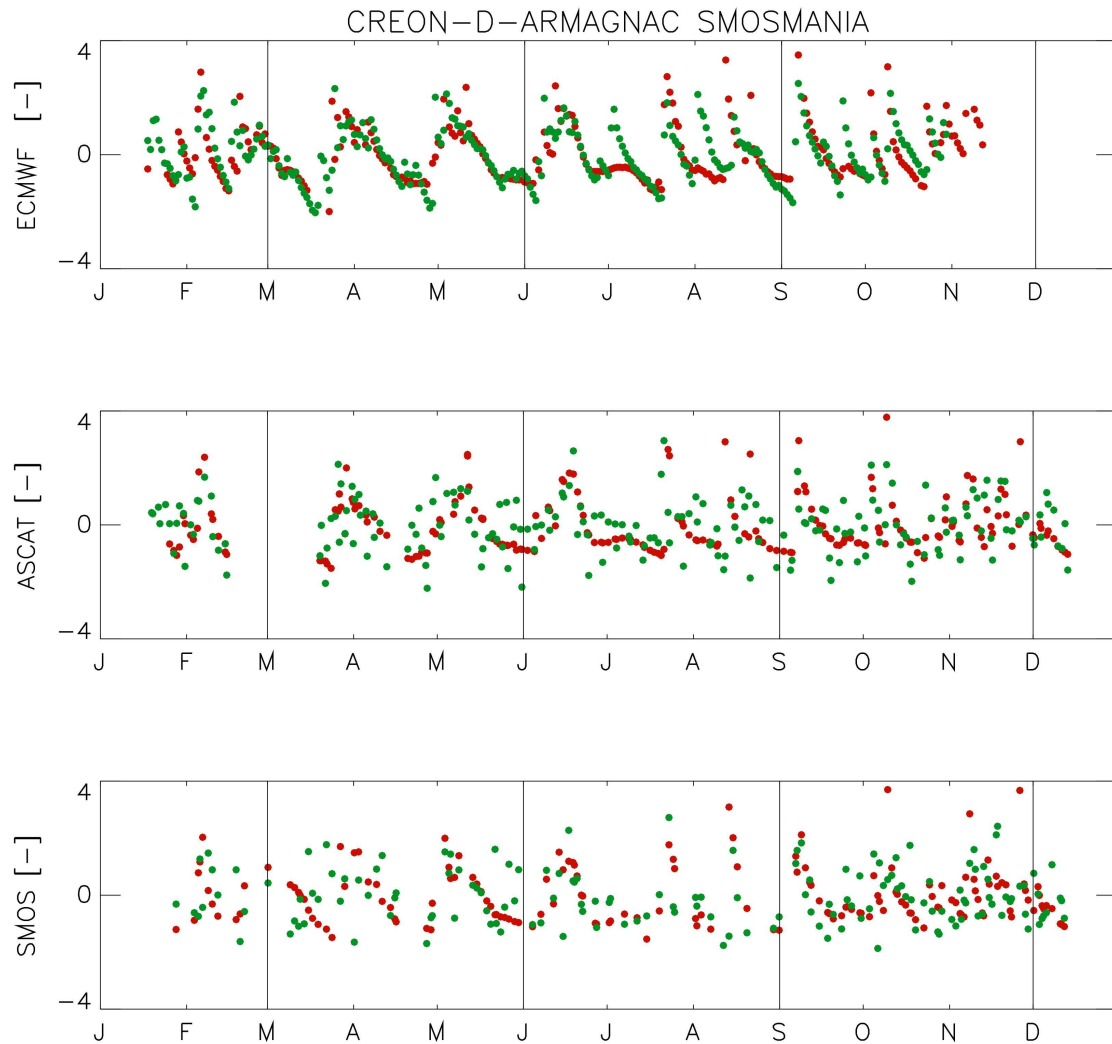


Figure 5.4: Temporal evolution of SSM anomaly time-series at the Creon d'Armagnac station of the SMOSMANIA network in southwestern France for 2010, from top to bottom; ECMWF (SM-DAS-2), ASCAT and SMOS (green dots). In situ anomaly time-series are in red.

Soil Moisture data set	Correlation [-]			Bias [-]			RMSD [-]		
	ECM	ASC	SMO	ECM	ASC	SMO	ECM	ASC	SMO
Normalised time series	0.71	0.55	0.55	-0.036	0.056	0.122	0.232	0.247	0.243
Anomaly time-series	0.57	0.45	0.43	-0.013	0.007	-0.013	0.824	0.967	1.001

Table 5.4: Comparisons between in situ SSM observations and products; SM-DAS-2 (ECM), ASCAT (ASC) and SMOS (SMO) for 2010. For normalised and anomaly time-series, mean correlation, bias (in situ minus analyses) and root mean square difference (RMSD) are given for each network and for each product. Scores are presented for stations presenting significant correlation levels (p-values ≤ 0.05) for all the three products. 168 and 165 stations for normalised and anomaly time-series, respectively, are available in this configuration.

correlation values show the same tendency but at a lower degree. Table 5.4 presents comparisons between ECM, ASC, SMO and in situ observations for the stations presenting significant levels of correlations (p-values < 0.05) for all the 3 products. Comparisons for normalised times-series as well as for anomaly time-series are presented. 168 and 165 stations for normalised and anomaly times-series, respectively, are available in this configuration. Evaluation of normalised time-series presents better scores than anomaly time series, R are 0.71, 0.55, 0.55 and 0.57, 0.45, 0.43 for ECM, ASC and SMO, respectively.

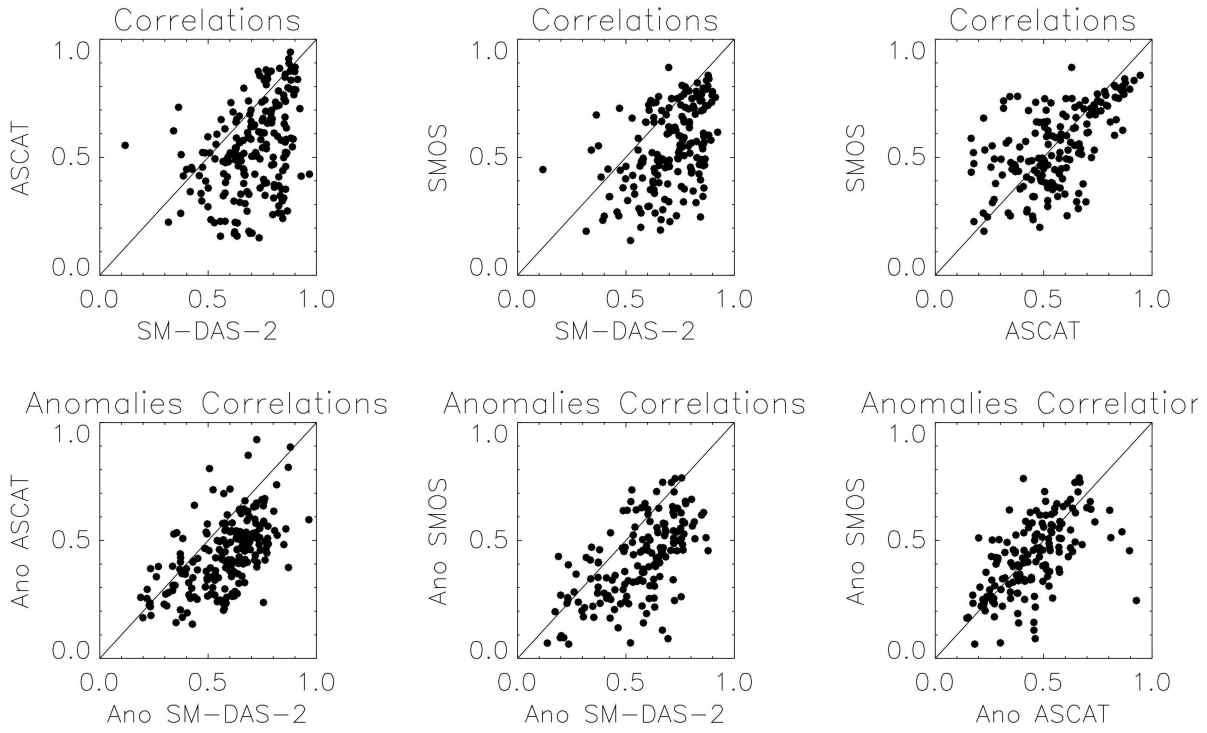


Figure 5.5: (top) correlations between ASCAT and in situ data against correlations between ECMWF SM-DAS-2 and in situ data, then same for SMOS and SM-DAS-2, SMOS and ASCAT. (Bottom) Same as top but for anomaly correlation values instead of normalised time series.

Chapter 6

Global comparison

General features of the products are compared, such as number and extreme values of observations. Then the soil moisture climatologies obtained from the three soil moisture products are compared, based on monthly maps, Hovmöller diagrams and latitudinal plots. Quantitative comparison results are provided by representing global maps of products correlation, root mean square difference for both volumetric and time series anomaly products.

6.1 Characteristics

Figure 6.1 presents the number of values and the standard deviation for the three products during 2010 (From the top to the bottom: SMOS, ASCAT and SM-DAS-2).

Global maps clearly show differences between the three products. SM-DAS-2 provides soil moisture value every day at global scale. In comparison ASCAT and SMOS provide a reduced number of observations. The number of value first depends on the orbit of the satellite. Then, all brightness temperatures (SMOS) and scatterometer coefficients (ASCAT) are not used by the retrieved algorithm. In addition, in this study, both product are filtered according to the results obtained in the previous chapter. Thus, few values or none are provided over equatorial forest because of the too high optical depth or over permafrost areas (frozen areas).

The standard deviation provide an information about the variability of soil moisture values provided by the products. Soil moisture standard deviation is similar for the three products over Africa, Arabic peninsula and Australia. Arabic and desert area in Africa are characterised by very low standard deviation, in accordance with bio-climatic conditions in these areas. Soil moisture standard deviation is in agreement over Sahelian area and over India according to the monsoon climatic system. At high latitudes (USA, Canada and Russia), SM-DAS-2 product provides much lower standard deviation values than ASCAT (SMOS being in intermediate position). In south America, soil moisture values from SM-DAS-2 and ASCAT are clearly more variable than those from SMOS.

Minimal and maximal soil moisture values provided by the three products are shown in Figure 6.2. The minimal value reached during 2010 by SMOS and ASCAT product is extremely close to 0 everywhere while SM-DAS-2 product is close to $0.2 \text{ m}^3.\text{m}^3$, and

also provides some areas with values higher than $0.5 m^3.m^3$.

The maximal value maps from SM-DAS-2 and ASCAT are particularly close because of the use of the saturation map. Thus, the main areas are close to $0.5 m^3.m^3$ except for Sahara and Arabic desert. SMOS product provides maximal soil moisture values between 0.3 and $0.6 m^3.m^3$ (except deserts). Values distribution is also more heterogeneous.

6.2 Monthly soil moisture values

Figure 6.3 presents the monthly mean soil moisture for the three products for January, April, and July. They show the main seasonal soil moisture characteristics at global scale. In January the three products are particularly different. SMOS is the only one not to provide soil moisture values over frozen areas at high latitudes. In these areas, values from SM-DAS-2 product are very high (about $0.3 m^3.m^3$) and those from ASCAT are low which can be realistic (soil partially frozen). In July, soil moisture conditions are very different from those in January. Soil are dryer in south hemisphere than in the north latitudes where the permafrost areas are also particularly wet for the three products. Map calculated for the months of April shows intermediate soil moisture distribution.

6.3 Latitudinal variations

Soil moisture distribution at global scale strongly depends on the latitude and season. Hovmöller diagrams are used here to illustrate seasonal variations of the longitudinal average of moisture values. Figure 6.4 shows Hovmöller plots (left) for the three products and corresponding averaged latitudinal profiles (right) for each quarter of 2010.

Hovmöller diagrams clearly show for the three products, the main variations of the soil moisture distribution at global scale. These areas correspond to the wettest areas on the plots. The first is the melting of the permafrost. On the hovmoller based on SMOS and ASCAT, soil moisture values strongly increase during the approximately day 150 to 250 (summer period in north hemisphere). SM-DAS-2 soil moisture values are high and the seasonal amplitude much lower than for SMOS and ASCAT, as shown by latitudinal profiles.

The second bioclimatic information is the moving of the ITCZ (InterTropical Convergence Zone). The three products provide this information as it can be seen on the hovmöller diagrams. The soil moisture values increase with latitude from DOY (Day Of Year) 50 to 230 and then decrease to reach than initial position.

SM-DAS soil moisture is particularly stable at high latitudes. This can be explained by the soil moisture values retrieved on the Greenland which is a very constant area.

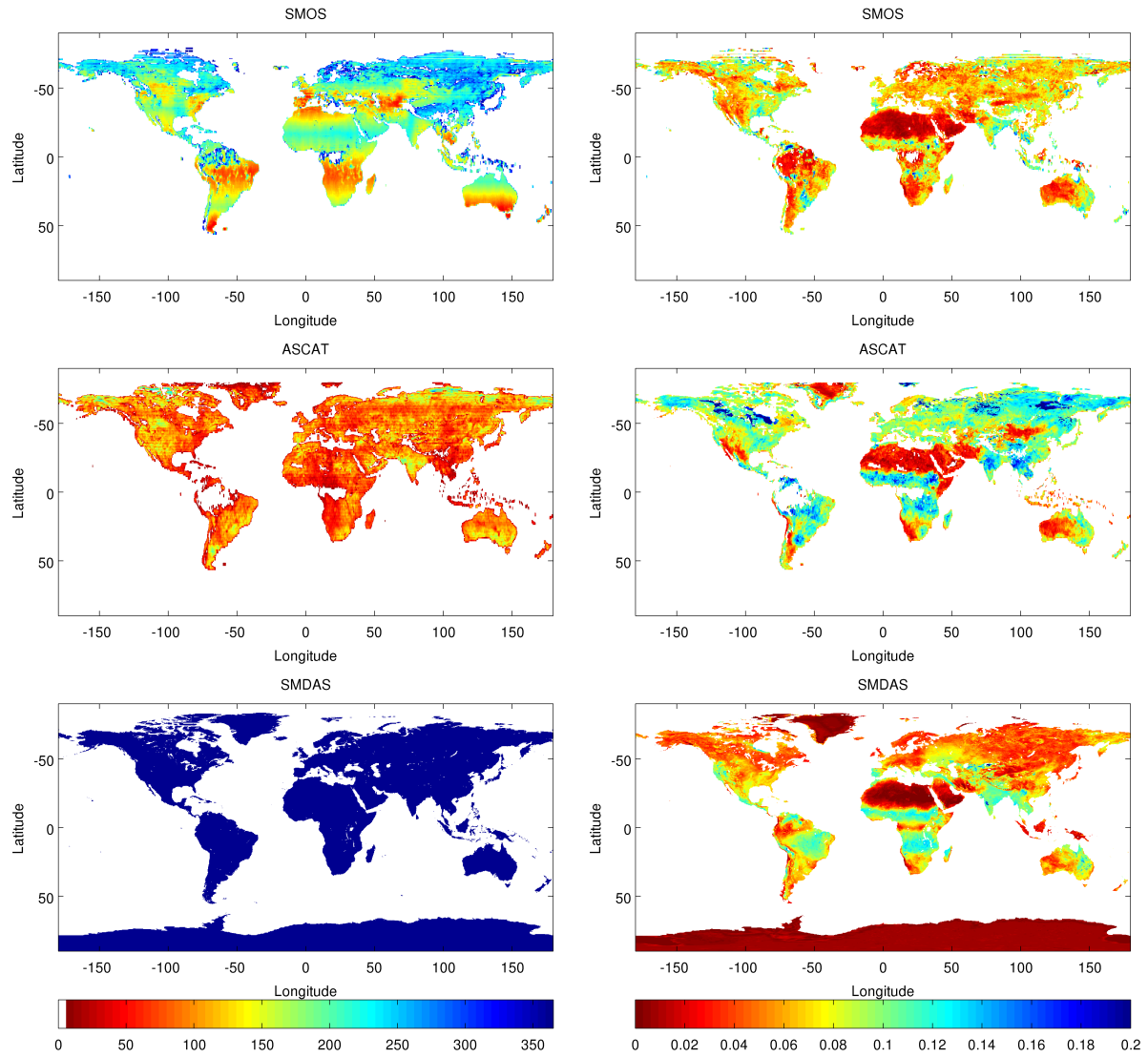


Figure 6.1: Number of observations (left) and soil moisture standard deviation $m^3.m^{-3}$ (right) for SMOS (top), ASCAT (middle), and SM-DAS-2 (bottom) for 2010.

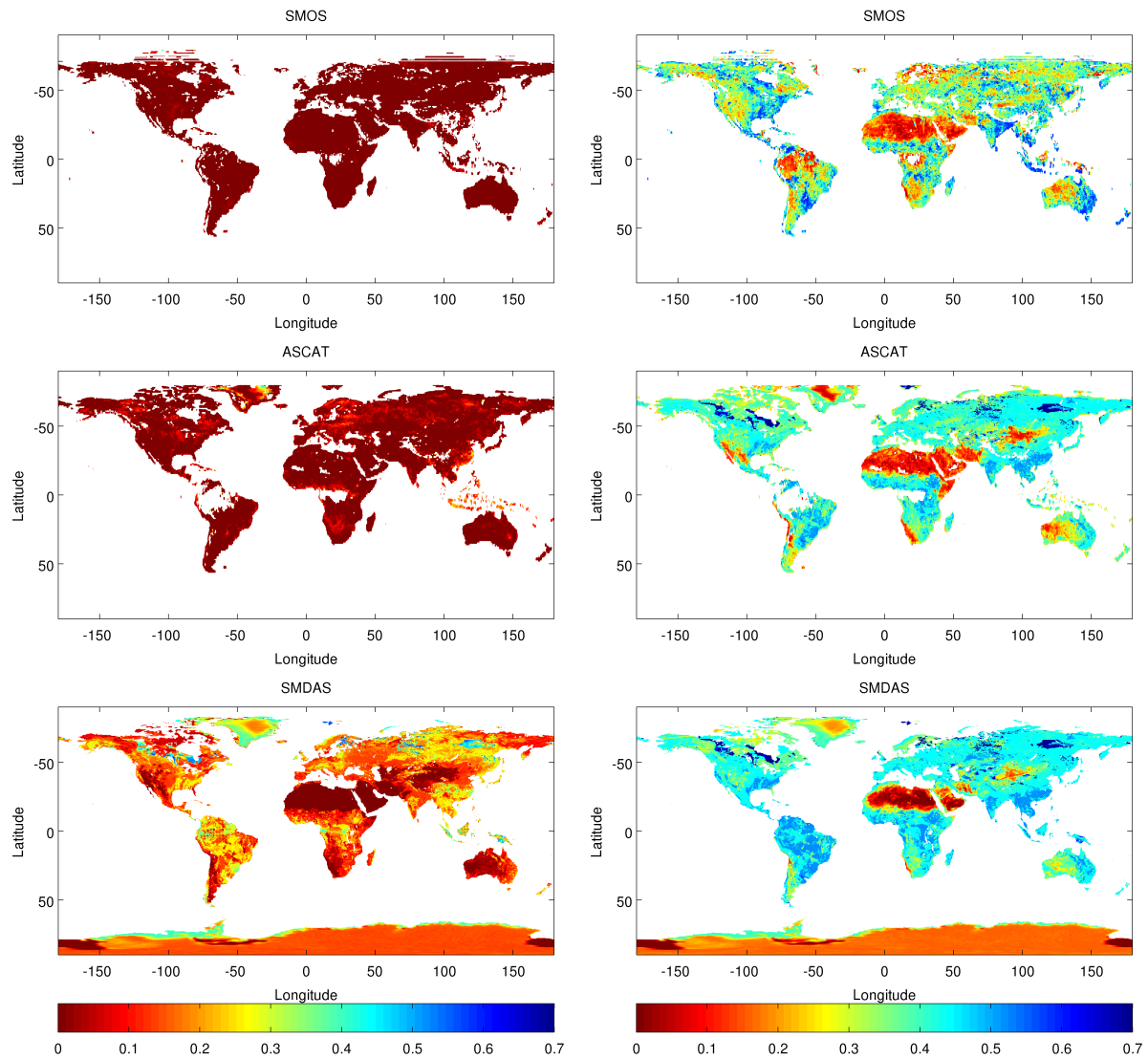


Figure 6.2: Minimal soil moisture in $m^3.m^{-3}$ (left) and maximal (right) values for SMOS (top), ASCAT (middle), and SM-DAS-2 (bottom) for 2010.

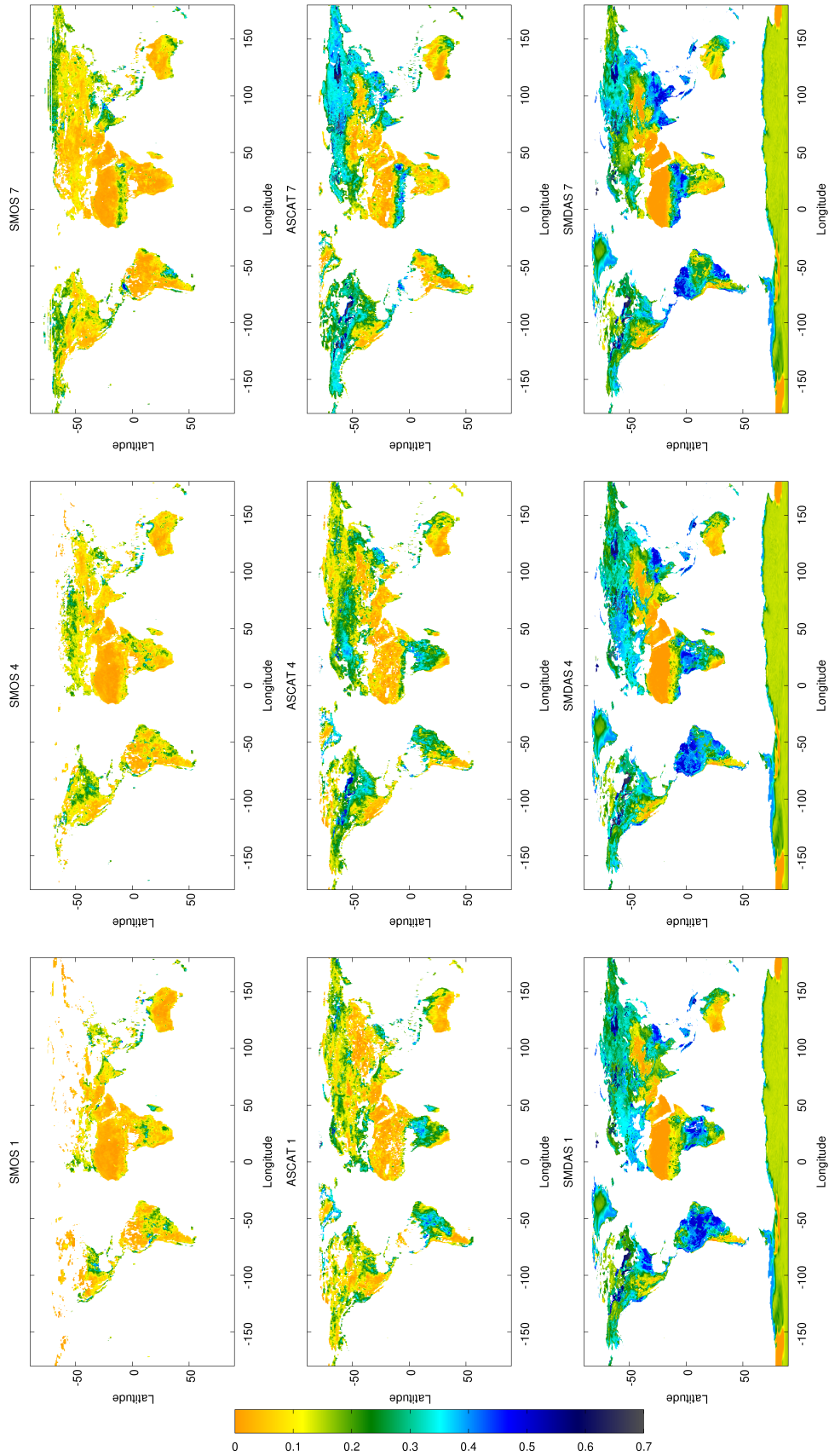


Figure 6.3: Monthly mean soil moisture ($m^3.m^{-3}$) for SMOS, ASCAT, and SM-DAS-2 for January, April, and July.

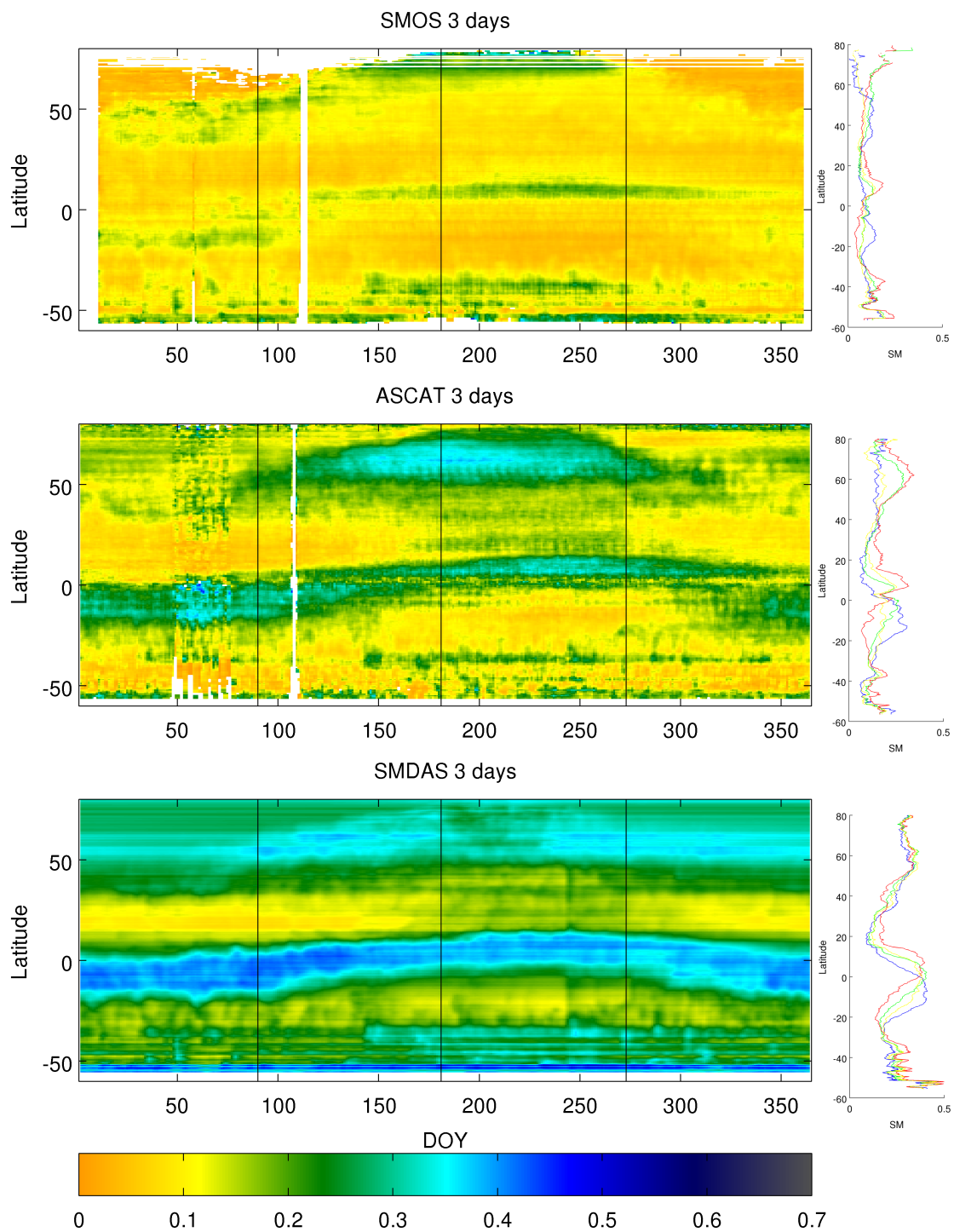


Figure 6.4: Left: Soil moisture time latitude variations (Hovmöller) for 2010, for SMOS (top), ASCAT (middle), and SM-DAS-2 (bottom). Time axis is represented with a three days moving window, and soil moisture values are longitudinal averaged. Right: Soil moisture latitudinal distribution for Jan-Feb-Mar (blue), Apr-May-Jun (green), Jul-Aug-Sep (yellow), and Oct-Nov-Dec (red). The black lines on the hovmoller plot correspond to the quarterly period.

6.4 Statistic results

This section presents quantitative comparison results between the three products at the annual scale. Correlation (R) and RMSD give information on agreement between the products (compared by pair), in term of seasonal dynamics and soil moisture range of variation. Maps of anomaly correlation evaluate the products consistency at short time scale independently from the annual cycle.

Figure 6.5 shows global anomaly correlation (right) and maps correlation (left) between the three pairs of products. The RMSD and related number of values available are shown by the Figure 6.6.

Statistical results presented show a significant adequacy between the temporal variations from all the products over Sahelian area, India and Australia. This result can be explained by the fact that these areas are subject to a strong seasonal annual cycle. Mean correlation ratio calculated on anomalies are clearly lower than with volumetric time series like for the RMSD (slightly higher for SM-DAS-2-ASCAT).

In Sahara, correlation values are very low, showing a very poor agreement between the three products in this area. This is due to the fact that soil moisture dynamic is very low, so variations are mostly related to signal noise, explaining low correlation between the products.

Different results can be observed on area with seasonal freezing. SMOS-ASCAT (top) is the only one pair of products to provide consistant temporal variation at annual scale. In contrast, this pair presents the more of inverse correlation about anomalies. Thus, the variations of soil moisture at short temporal scale, link to precipitations, are not similarly detected.

Statistical results was averaged over several areas. These areas are selected according to their representativity of different bioclimatic conditions. They are located in North and South America, Africa, Russia and Australia as shown by the Figure 6.7. Table 6.1 presents the statistical results showing a large heterogeneity between products and areas. The more significant adequacy is obtained between the ASCAT and SM-DAS-2 product in term of annual variability over South America where the R value reaches 0.6478. However, this adequacy is mainly explained by the coherency of both seasonal cycles. Indeed, the correlation ratio obtained between both anomalies series is not as well (0.1302). It is over Australia area where the correlation ratio on anomalies series is the highest with 0.2884.

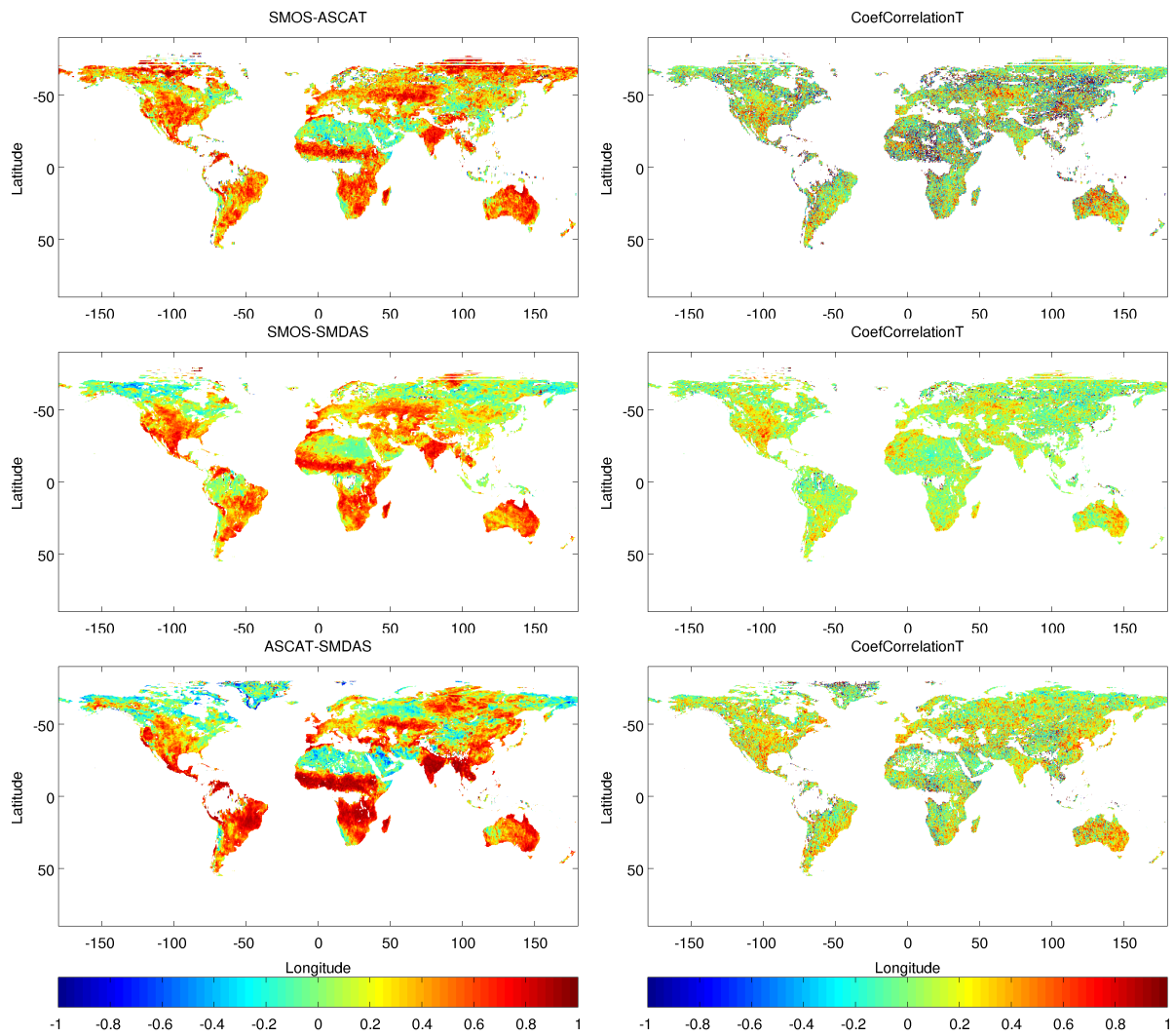


Figure 6.5: Global maps correlation (left) and anomaly correlation (right) between the three pairs of products (Top: SMOS-ASCAT, Middle: SMOS-SM-DAS and bottom: ASCAT-SM-DAS).

Area	SMOS-ASCAT			SMOS-SM-DAS-2			SM-DAS-2-ASCAT		
	R_{vol}	R_{ano}	RMSD	R_{vol}	R_{ano}	RMSD	R_{vol}	R_{ano}	RMSD
North America	0.5318	0.2107	0.1270	0.5056	0.2583	0.1343	0.3950	0.2553	0.1932
South America	0.4445	0.1115	0.0900	0.4156	0.0705	0.0857	0.6478	0.1302	0.2048
Africa	0.4163	0.1398	0.0801	0.4601	0.0499	0.0730	0.5445	0.0817	0.1473
Russia	0.3015	0.0894	0.1112	0.1879	0.0589	0.1095	0.2703	0.1373	0.2146
Australia	0.5056	0.2607	0.0683	0.4482	0.1734	0.0701	0.4578	0.2884	0.1080

Table 6.1: Regional scale statistics obtained for 2010 for the products comparison by pair. Regions are defined as shown in Figure 6.7.

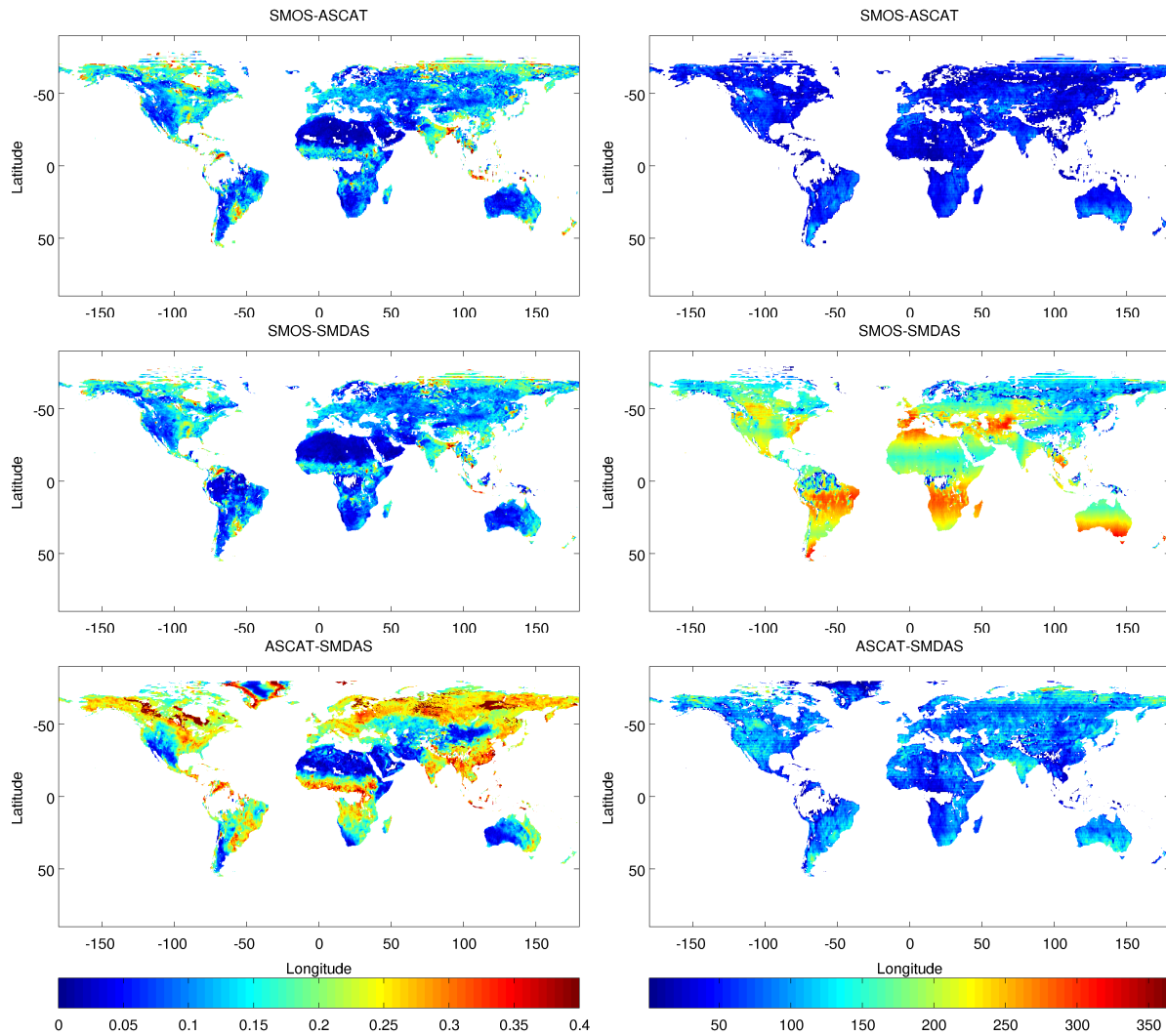


Figure 6.6: Global maps RMSD (left) and number of day with available values from both products (right) between the three pairs of products (Top: SMOS-ASCAT, Middle: SMOS-SM-DAS and bottom: ASCAT-SM-DAS).

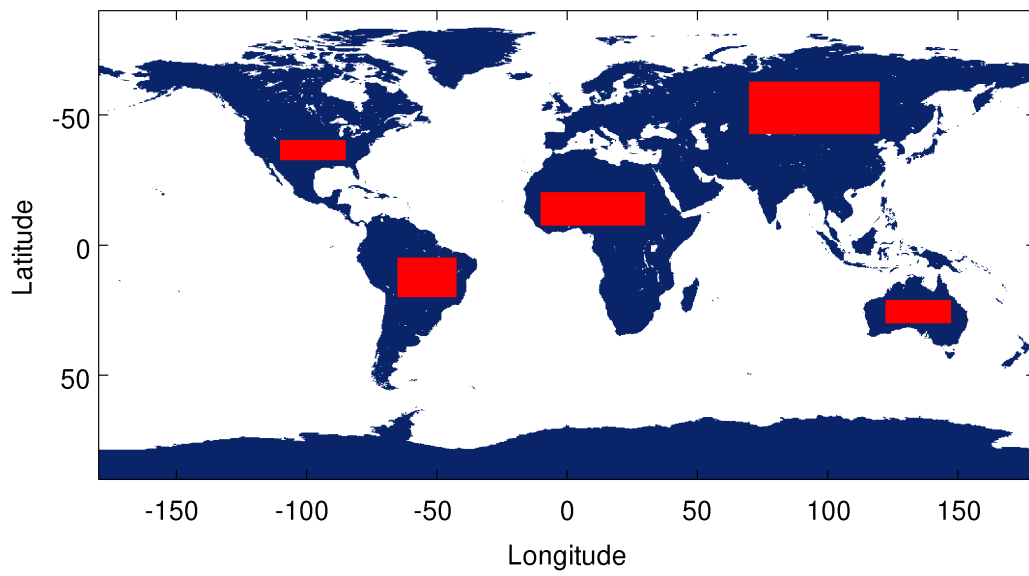


Figure 6.7: Selected area for regional scale comparison (cf. Table 6.1).

Chapter 7

Conclusion

In this report three global products of surface soil moisture were compared at local, regional and global scales for the year 2010.

- SMOS level 2 surface soil moisture is a remotely sensed product. It is based on L-band passive measurements of the Earth emission. SMOS retrieval algorithm uses multi-angular SMOS measurements that allow to filter out vegetation contribution to the signal. SMOS soil moisture is an ESA/CESBIO product. It is a swath global product with a mean revisit time of 3 days and a resolution of about 40km.
- ASCAT level 2 surface soil moisture is a remotely sensed product, based on C-band active measurements of backscattering coefficient. ASCAT retrieval algorithm was developed and it is supported by TU-Wien. ASCAT soil moisture is an H-SAF product (SM-OBS-1), produced operationally by EUMETSAT CAF. It is a global dual swath product with a mean revisit time of 3 days and a resolution of about 25km.
- SM-DAS-2 soil moisture is a data assimilation product. It is based on the ECMWF land data assimilation system which derives, from ASCAT surface soil moisture data assimilation, soil moisture at surface and in the root zone. Data assimilation optimally combines ASCAT and other types of information (screen level temperature and relative humidity). SM-DAS-2 is an H-SAF product developed, supported and produced by ECMWF. It is provided with a daily global coverage at 25km resolution.

To evaluate the reliability of the three soil moisture products, local in situ surface soil moisture data sets from more than 200 stations were used as ground truth. Stations are located in Africa, Australia, Europe and United States. Results show general good performances of the three products to capture surface soil moisture annual cycle as well as short term variability. Correlation values between the data sets are very satisfactory over most of the investigated sites, located in contrasted biomes and climate conditions with averaged values of 0.70 for SM-DAS-2, 0.53 for ASCAT (SM-OBS-1) and 0.54 for SMOS. SM-DAS-2 soil moisture analysis performances were found rather similar across the different studied sites with the exception of Western Africa presenting lower correlations. For this product, an estimate of the average error is about $0.07 \text{ m}^3.\text{m}^{-3}$. SM-DAS-2 provides, for the first time, a global daily product of consistent quality of surface soil moisture index,

available in near real time. Such product is required for many applications to be used as realistic initial states for the soil moisture variables, from forecasts of weather and seasonal climate variations to models of plant growth and carbon fluxes. ASCAT (SM-OBS-1) and SMOS present similar performances with an estimated error of $0.08 \text{ m}^3.\text{m}^{-3}$ on average for all the considered stations. Concerning SMOS, it is interesting to note that results are already of very good quality for a recently launched satellite. SMOS retrieval algorithm have been continuously improving in the past months and SMOS products quality are expected to be greatly improved in the near future.

Global scale comparison between the products showed that in terms of number of observations, SM-DAS-2 provides a uniform daily global coverage, with 365 values per day on every land pixel. In contrast the two remote sensing products have a non-uniform coverage related to the satellite orbits and data filtering at both the retrieval level and data use of quality index. ASCAT soil moisture is masked in tropical forests, mountainous areas and wetlands, using data quality index filtering and SMOS is filtered for soil moisture quality index larger than $0.045 \text{ m}^3.\text{m}^{-3}$.

In terms of soil moisture range, global maps of minimum and maximum soil moisture values show that (i) ASCAT and SMOS have a very consistent minimum value (2) and to a less extent ASCAT and SM-DAS-2 present consistent maps of maximum soil moisture. Minimum values for SMOS indicate that completely dry conditions (with $0 \text{ m}^3.\text{m}^{-3}$) are reached everywhere at least once in 2010. This is consistent with local scale validation results for SMOS which showed general underestimation of soil moisture by this product. ASCAT dry conditions are also very extreme and apart from Indonesia, completely dry conditions are also reached at almost every location. The relative consistency between SM-DAS-2 and ASCAT maximum soil moisture value is influenced by the fact that the two products were converted into volumetric values using the same maximum reference. However it is coherent with global bioclimatic conditions, with for instance maximum soil moisture values close to $0.45 \text{ m}^3.\text{m}^{-3}$ in the H-SAF area.

The analysis of soil moisture seasonal cycles show significant differences between the products. Monthly maps show that SMOS has small seasonal variations between 50°S and 60°N , with larger monthly variations at very high latitudes (north of 60°N). ASCAT shows most contrasted monthly maps with large differences between January and July monthly mean soil moisture, at high latitude and in temperate area as well as in tropical regions. SM-DAS-2 also presents large seasonal differences in temperate and tropical areas. In contrast to ASCAT it has relatively constant monthly mean soil moisture values at high latitudes (north of 50°N).

Seasonal latitudinal soil moisture variations are well illustrated by Hovmöller diagrams which confirm that, when averaged on all longitudes, SMOS present consistently dry soil moisture conditions (less than $0.15 \text{ m}^3.\text{m}^{-3}$) at all latitudes, except north of 60°N , and all seasons. ASCAT SM-OBS-1 captures seasonal variations in the inter tropical area and in the northern hemisphere at latitudes above 50°N . Soil moisture variations in the inter tropical area results from the seasonal movement of the meteorological equator which is associated to high precipitation in the Inter Tropical Convergence Zone. In high latitudes, summer is associated to wetter soil moisture conditions than in winter when frozen conditions reduce the liquid soil moisture content (measured from remote sensors). SM-DAS-2

also presents very strong seasonal cycle variations in the ITCZ and in mid-latitude up to 50 °N. However, compared to ASCAT, SM-DAS-2 has much lower soil moisture seasonal variations above 50 °N where wet conditions are represented all the year along.

Correlation and RMSD between the products by pair of two were also analysed at global and regional scale. Results show that the three products are in general good agreement in the Sahelian area, over India and eastern Australia. Anomaly correlation maps show poorer agreement between the products at short time scale, in agreement with results obtained at local scale.

The three products evaluated and compared in this report are all in continuous developments. The SM-DAS-2 production chain is being improved within the H-SAF project, to better account for snow processes in the data assimilation system. The SMOS retrieval algorithm is under improvements to better filter out RFI that affect the brightness temperature data. ASCAT SM-OBS-1 operational algorithm was improved in August 2011, increasing the number of data while improving the soil moisture product quality and quality flag use. So, products performances presented here against ground stations are expected to be further improved in the next few year for the three products.

Bibliography

- Albergel, C., J.-C. Calvet, P. de Rosnay, G. Balsamo, W. Wagner, S. Hasenauer, V. Naemi, E. Martin, E. Bazile, F. Bouyssel, and J.-F. Mahfouf, 2010 : Cross-evaluation of modelled and remotely sensed surface soil moisture with in situ data in southwestern france. *Hydrol. Earth Syst. Sci.*, **14**,2177–2191.
- Albergel, C., C. Rüdiger, D. Carrer, J.-C. Calvet, N. Fritz, V. Naeimi, Z. Bartalis, and S. Hasenauer, 2009 : An evaluation of ascat surface soil moisture products with in situ observations in southwestern france. *Hydrol. Earth Syst. Sci.*, **13**,115â124.
- Albergel, C., C. Rüdiger, T. Pellarin, J.-C. Calvet, N. Fritz, F. Froissard, D. Suquia, D. Petitpa, B. Pignatelli, and M. E., 2008 : From near-surface to root-zone soil moisture using an exponential filter: an assessment of the method based on in situ observations and model simulations. *Hydrol. Earth Syst. Sci.*, **12**,1323â1337.
- Albergel, C., E. Zakharova, J.-C. Calvet, M. Zribi, M. Pardé, J.-P. Wigneron, N. Novello, Y. Kerr, M. A., and N. Fritz, 2011 : A first assessment of the smos data in southwestern france using in situ and airborne soil moisture estimates: the carols airborne campaign. *Remote sens. environ.*, **115**,2718–2728.
- Balsamo, G., P. Viterbo, A. Beljaars, B. van den Hurk, M. Hirschi, A. Betts, and S. K., 2009 : A revised hydrology for the ecmwf model: Verification from field site to terrestrial water storage and impact in the ecmwf-ifs. *J. Hydrometeorol.*, **10**,623â643.
- Bartalis, Z., S. Hasenauer, V. Naeimi, and W. Wagner, 2007a : Warp-nrt 2.0 reference manual. *ASCAT Soil Moisture Report Series, Institute of Photogrammetry and Remote Sensing, Vienna University of Technology*, **14**.
- Bartalis, Z., W. Wagner, V. Naeimi, S. Hasenauer, K. Scipal, H. Bonekamp, J. Figa, and C. Anderson, 2007b : Initial soil moisture retrievals from the metop-a advanced scatterometer (ascat). *Geophys. Res. Lett.*, **34**,L20401.
- Brocca, L., S. Hasenauer, T. Lacava, F. Melone, T. Moramarco, W. Wagner, W. Dorigo, P. Matgen, J. Martínez-Fernández, P. Llorens, J. Latron, C. Martin, and M. Bittelli, 2011 : Soil moisture estimation through ascat and amsr-e: An intercomparison and validation study across europe. *Remote sens. environ.*
- Brocca, L., F. Melone, T. Moramarco, W. Wagner, and S. Hasenauer, 2010a : Ascat soil wetness index validation through in situ and modelled soil moisture data in central italy. *Remote sens. environ.*, **114**(11),2745–2755.

- Brocca, L., F. Melone, T. Moramarco, W. Wagner, V. Naeimi, Z. Bartalis, and S. Hasenauer, 2010b : Improving runoff prediction through the assimilation of the ascat soil moisture product. *Hydrol. Earth Syst. Sci.*, **14**,2745–2755.
- Calvet, J.-C., P. Bessemoulin, J. Noilhan, C. Berne, I. Braud, D. Courault, N. Fritz, E. Gonzalez-Sosa, J. Goutorbe, R. Haverkamp, G. Jaubert, L. Kergoat, G. Lachaud, J. Laurent, P. Mordélet, A. Olioso, P. Peris, J. Roujean, J. Thony, C. Tosca, M. Vauclin, and D. Vignes, 1999 : MUREX: a land-surface field experiment to study the annual cycle of the energy and water budgets. *Ann. Geophys.*, **17**,838–854.
- de Rosnay, P., M. Drusch, G. Balsamo, I. L., and C. Albergel, 2011 : Extended Kalman Filter soil moisture analysis in the IFS. *ECMWF Spring Newsletter*, **127**,12–16.
- de Rosnay, P., C. Gruhier, F. Timouk, F. Baup, E. Mougin, P. Hiernaux, L. Kergoat, and V. LeDantec, 2009 : Multi-scale soil moisture measurements at the Gourma meso-scale site in Mali. *J. Hydrol.*, **375**.
- Dharssi, I., K. Bovis, B. Macpherson, and J. C., 2011 : Operational assimilation of ascat surface soil wetness at the met office. *Hydrol. Earth Syst. Sci. Discuss.*, **8**,4313–4354.
- Dorigo, W., W. Wagner, R. Hohensinn, S. Hahn, C. Paulik, M. Drusch, S. Mecklenburg, P. van Oevelen, A. Robock, and T. Jackson, 2011 : The international soil moisture network: a data hosting facility for global in situ soil moisture measurements. *Hydrol. Earth Syst. Sci.*, **15**,1675–1698.
- Draper, C., J.-F. Mahfouf, J.-C. Calvet, E. Martin, and W. Wagner, 2011 : Assimilation of ascat near-surface soil moisture into the french sim hydrological model. *Hydrol. Earth Syst. Sci. Disc.*, **8**,5427–5464.
- Drusch, M., K. Scipal, P. de Rosnay, G. Balsamo, E. Anderson, P. Bougeault, and P. Viterbo, 2009 : Towards a kalman filter based soil moisture analysis system for the operational ecmwf integrated forecast system. *Geophys. Res. Lett.*, **36**,L10401.
- Gruhier, C., P. de Rosnay, S. Hasenauer, T. Holmes, R. de Jeu, Y. Kerr, E. Mougin, E. Njoku, F. Timouk, W. Wagner, and M. Zribi, 2010 : Soil moisture active and passive microwave products: intercomparison and evaluation over a Sahelian site. *Hydrology and Earth System Sciences*, **14**,141–156.
- Hahn, S., and W. Wagner, 2011 : Characterisation of calibration-related errors on the initial metop ascat soil moisture product. *Geophysical Research Abstract*, **13**,EGU2011–3178.
- Jackson, T., A. Hsu, A. van de Griend, and J. Eagleman, 2004 : Skylab L band microwave radiometer observations of soil moisture revisited. *Int. J. Remote Sens.*, **25**,2585–2606.
- Kerr, Y., 2007 : Soil Moisture from space: Where we are ? *Hydrogeology journal*, **15**,117–120.

- Kerr, Y., P. Waldteufel, P. Richaume, J. Wigneron, P. Ferrazzoli, and R. Gurney, 2007 : Smos level 2 processor for soil moisture - algorithm theoretical based document (atbd). Technical report, Hadley Centre Climate research technical note CRNT 59, CBSA, SO-TN-ESL-SM-GS-0001, Issue 3.a. 129 p.
- Kerr, Y., P. Waldteufel, J.-P. Wigneron, S. Delwart, F. Cabot, J. Boutin, M.-J. Escorihuela, J. Font, N. Reul, C. Gruhier, S. Juglea, M. Drinkwater, A. Hahne, M. Martiñe-Neira, and S. Mecklenburg, 2010 : The SMOS Mission: New Tool for Monitoring Key Elements of the GlobalWater Cycle. *Proceedings of the IEEE*, **98** (5),666–687.
- Loew, A., J. Dall’Amico, F. Schlenz, and W. Mauser, 2010 : The upper danube soil moisture validation site: measurements and activities. *Earth Observation and Water Cycle conference, Frascati (Rome), 18-20 November 2009, ESA Special Publication SP-674*.
- Lopez, P., 2011 : Direct 4d-var assimilation of ncep stage iv radar and gauge precipitation data at ecmwf. *Monthly Weather Rev.*, **139**,2098–2116.
- Mahfouf, J.-F., 2010 : Assimilation of satellite-derived soil moisture from ascat in a limited-area nwp model. *Q. J. R. Meteorol. Soc.*, **136**,784–198.
- Martínez-Fernández, J., and A. Ceballos, 2005 : Mean soil moisture estimation using temporal stability analysis. *J. Hydrol.*, **312** (1-4),28â38.
- Njoku, E., T. Jackson, V. Lakshmi, T. Chan, and S. Nghiem, 2003 : Soil moisture retrieval from AMSR-E. *IEEE Geosc. Remote Sens. Let.*, **41**(2),215–229.
- Parinussa, R. M., T. R. H. Holmes, and W. T. Crow, 2011 : The impact of land surface temperature on soil moisture anomaly detection from passive microwave observations. *Hydrol. Earth Syst. Sci. Discuss.*, **8**.
- Pellarin, T., J. Laurent, B. Cappelaere, B. Decharme, D. L., and D. Ramier, 2009a : Hydrological modelling and associated microwave emission of a semi-arid region in South-western Niger. *J. Hydrol.*, **375**,262–272.
- Pellarin, T., T. Tran, J.-M. Cohard, S. Galle, J.-P. Laurent, P. de Rosnay, and T. Vischel, 2009b : Soil moisture mapping over West Africa with a 30-min temporal resolution using AMSR-E observations and a satellite-based rainfall product. *Hydrol. Earth Syst. Sci.*, **13**,1887â1896.
- Redelsperger, J.-L., C. Thorncroft, A. Diedhiou, T. Lebel, D. Parker, and J. Polcher, 2006 : African Monsoon, Multidisciplinary Analysis (AMMA): An International Research Project and Field Campaign. *Bull. Amer. Meteorol. Soc*, **87**(12),1739–1746.
- Rüdiger, C., J.-C. Calvet, C. Gruhier, T. R. H. Holmes, R. A. M. de Jeu, and W. Wagner, 2009 : An Intercomparison of ERS-Scat and AMSR-E Soil Moisture Observations with Model Simulations over France. *American Meteorological Society*, **10**,431–447.

- Sabater, J., C. Rötter, J.-C. Calvet, N. Fritz, L. Jarlan, and Y. Kerr, 2008 : Joint assimilation of surface soil moisture and LAI observations into land surface model. *Agricultural and Forest Meteorology*, **148**,1362–1373.
- Schaefer, G., and R. Paetzold, 2000 : Snotel (snowpack telemetry) and scan (soil climate analysis network). *Automated Weather Station (AWS) workshop*, pp. March 6–10. Lincoln, NE.
- Schmugge, T., 1983a : Remote sensing of soil moisture: Recent advances. *IEEE Trans. Geosc. Remote Sens.*, **21(3)**,336–344.
- Schmugge, T. J., 1983b : Remote sensing of soil moisture: recent advances. *IEEE Trans. Geosc. Remote Sens.*, **GE21**,145–146.
- Scipal, K., M. Drusch, and W. Wagner, 2008 : 2008: Assimilation of a ers scatterometer derived soil moisture index in the ecmwf numerical weather prediction system. *Advances in water resources*, **31(8)**,1101–1112.
- Taylor, K., 2001 : Summarizeing multiple aspects of model performance in a single diagram. *J. Geophys. Res.*, **106**,7183–7192.
- van den Hurk, B., and P. Viterbo, 2003 : The torne-kalix pilps 2e experiment as a test bed for modifications to the ecmwf land surface scheme. *Global and Planetary Change*, **38**,165–173.
- Wagner, W., Z. Bartalis, V. Naeimi, S.-E. Park, J. Figa-Saldaña, and H. Bonekamp, 2010 : Status of the metop ascat soil moisture product. *Geoscience and Remote Sensing Symposium 2010 (IGARSS2010)*, **25-30 July 2010, Honolulu, Hawaii, U.S.A.**,276–279.
- Wagner, W., G. Lemoine, and H. Rott, 1999 : A method for estimating soil moisture from ers scatterometer and soil data. *Remote sens. environ.*, **70(2)**,191–207.
- Wagner, W., V. Naeimi, K. Scipal, R. de Jeu, and J. Martínez-Fernández, 2007 : Soil moisture from operational meteorological satellites. *Hydrogeology Journal*, **15(1)**,121–131.
- Waldteufel, P., and J.-L. Vergely, 2003 : Soil moisture retrieval for the smos mission. *Retrieval Algorithm Document, ACRI-ST, Sophia antipolis, Technical note SMOS-TN-ACR-SA-002, 25/03/2003*.
- Walker, J. P., G. R. Willgoose, and J. D. Kalma, 2001 : Assimilation of near-surface observations: A comparison of retrieval algorithms. *Advances in Water Resources*, **24(6)**,631–650.
- Wigneron, J.-P., A. Chanzy, J.-C. Calvet, and N. Bruguier, 1995 : A simple algorithm to retrieve soil moisture and vegetation biomass using passive microwave measurements over crop fields. *Remote sens. environ.*, **51**,331–341.

- Wigneron, J.-P., P. Waldteufel, A. Chanzy, J.-C. Calvet, and Y. Kerr, 2000 : Two - d microwave interferometer retrieval capabilities over land surfaces (smos mission). *Remote sens. environ.*, **73(3)**,270–282.
- Young, R., J. Walker, N. Yeoh, A. Smith, K. Ellett, M. O., and A. Western, 2008 : Soil moisture and meteorological observations from the murrumbidgee catchment. *Department of Civil and Environmental Engineering, The University of Melbourne.* (<http://www.oznet.org.au/mdbdata/document.html>, last access, 10/05/2011), pp. 16553–16578.
- Zribi, M., M. Pardé, J. Boutin, P. Fanise, D. Hauser, M. Dechambre, Y. Kerr, M. Leduc-Leballeur, M. Skou, S. Sobjaerg, C. Albergel, J.-C. Calvet, J.-P. Wigneron, E. Lopez-Baeza, K. Saleh, A. Ruis, and J. Tenerelli, 2011 : Land and ocean calibration and validation of smos: the carols airborne campaigns. *Sensors*, **11**,719–742.